Spectrum of Extratesticular and Testicular Pathologic Conditions at Scrotal MR Imaging[1]

Pardeep K. Mittal, MD
Ahmed S. Abdalla, MD
Argha Chatterjee, MD
Deborah A. Baumgarten, MD, MPH
Peter A. Harri, MD
Jay Patel, MD
Courtney C. Moreno, MD
Helena Gabriel, MD
Frank H. Miller, MD

Abbreviations: ADC = apparent diffusion coefficient, AFP = α-fetoprotein, MGCT = mixed germ cell tumor, WHO = World Health Organization

RadioGraphics 2018; 38:806–830

https://doi.org/10.1148/rg.2018170150

Content Codes: GU MR OI US

[1]From the Department of Radiology and Imaging Sciences, Emory University School of Medicine, Atlanta, Ga (P.K.M., D.A.B., P.A.H., J.P., C.C.M.); Department of Clinical Imaging, Hamad Medical Corporation, Doha, Qatar (A.S.A.); and Department of Radiology, Northwestern University Feinberg School of Medicine, Chicago, Ill (A.C., H.G., F.H.M.). Presented as an education exhibit at the 2016 RSNA Annual Meeting. Received May 29, 2017; revision requested August 10 and received August 25; accepted September 1. For this journal-based SA-CME activity, the authors, editor, and reviewers have disclosed no relevant relationships. **Address correspondence to** P.K.M., Department of Radiology and Imaging, Medical College of Georgia, 1120 15th St, Augusta, GA 30912 (e-mail: *pmittal@augusta.edu*).

SA-CME LEARNING OBJECTIVES

After completing this journal-based SA-CME activity, participants will be able to:

- Discuss the spectrum of benign and malignant extratesticular and testicular pathologic conditions at MR imaging.
- Recognize the testicular pathologic conditions for which MR imaging plays a crucial problem-solving role.
- Describe relevant MR imaging techniques and the utility of various sequences for imaging of scrotal lesions.

See www.rsna.org/education/search/RG.

Contact information that appeared in the print version of this article was updated in the online version on May 14, 2018.

Diagnostic workup of scrotal lesions should begin with a complete clinical history and physical examination, including analysis of risk factors such as family history of testicular cancer, personal history of tumor in the contralateral testis, and cryptorchidism, followed by imaging. Scrotal ultrasonography (US) with a combination of gray-scale and color Doppler techniques has been the first-line imaging modality for evaluation of testicular and extratesticular lesions because of its low cost, wide availability, and high diagnostic accuracy. However, US has limitations related to operator dependence, the relatively small field of view, and lack of tissue characterization. Magnetic resonance (MR) imaging, because of its superior soft-tissue contrast and multiplanar capabilities, is increasingly being used as a supplemental diagnostic problem-solving tool in cases where scrotal US findings are inconclusive or nondiagnostic. In addition to morphology, lesion location, and tissue characterization (eg, fat, blood products, granulation tissue, and fibrosis), scrotal MR imaging provides important information that can affect surgical planning and improve patient care. MR imaging also is helpful for differentiating testicular and extratesticular lesions, distinguishing between benign and malignant lesions, and evaluating the local extent of disease. This review discusses the anatomy and MR imaging features of testicular and extratesticular neoplastic and nonneoplastic conditions and describes relevant MR imaging techniques.

Introduction

Along with clinical examination, imaging plays an important role in the assessment of testicular and extratesticular lesions. Scrotal ultrasonography (US) remains the modality of choice for evaluation of scrotal pathologic conditions because of its wide availability, low cost, and high sensitivity for detection of scrotal lesions. However, in certain cases, characterization of testicular and extratesticular lesions at US is limited because of operator dependence, the small field of view, and limited tissue characterization. Magnetic resonance (MR) imaging of the scrotum has been proposed as an alternative problem-solving technique in cases of inconclusive, equivocal, or nondiagnostic US findings. The role of MR imaging is summarized in Figure 1 (1). MR imaging is a useful diagnostic tool for anatomic and morphologic assessment because of its multiplanar capabilities, including simultaneous imaging of the testicular and extratesticular spaces, and for tissue characterization because of the superior soft-tissue contrast. To ensure adequate treatment planning, it is important to determine the accurate location of scrotal lesions as either testicular or extratesticular (1). Most extratesticular masses are benign, and radical orchiectomy may be avoided. Testicular masses are considered malignant until proven otherwise, but scrotal MR imaging with a multiparametric approach helps narrow the differential diagnosis

TEACHING POINTS

- Sinus or fistulous tracts in tuberculosis occur as a result of a caseous abscess reaching the skin; a chronic draining sinus tract should be considered of tuberculous origin unless proven otherwise.
- Tuberculosis and fungal infections should be considered in the differential diagnosis for sclerosing lipogranuloma. Necrotic material may be seen in these conditions; multinucleated giant cells with fat vacuoles are diagnostic for sclerosing lipogranuloma.
- Serial follow-up of traumatic testicular lesions should be performed because up to 15% of tumors can be detected after episodes of trauma. Traumatic lesions tend to resolve, whereas tumors continue to grow.
- At MR imaging, the normal testis has homogeneous intermediate T1 signal intensity and high T2 signal intensity and is surrounded by a fibrous layer of tunica albuginea, which has low T1 and T2 signal intensity. In the context of a hematoma, areas of heterogeneous low T2 signal intensity raise the possibility of testicular injury, and interruption of the low-signal-intensity line representing the tunica albuginea is the key finding of testicular rupture; therefore, it is important to evaluate the tunica albuginea in all three imaging planes.
- Inflammatory processes such as epididymo-orchitis are tender at physical examination but improve after treatment with antibiotics, whereas lymphoma or other testicular tumors are painless and do not resolve after treatment but can demonstrate interval growth. Testicular sarcoid is more common in African-American males and does not respond to antibiotics. Testicular lymphoma can be an infiltrative process and can affect patients with a previous history of leukemia.

for both extratesticular and testicular lesions. It also helps determine precise treatment strategies in cases where surgical exploration and orchiectomy can be avoided and conservative treatment, clinical and imaging follow-up, biopsy, or testicular-sparing surgery can be performed (1–3).

MR Imaging

Imaging Protocol and Normal Appearance of the Testes

Scrotal MR imaging should be performed with a 1.5-T magnet and a phased-array surface coil, and the testes should be elevated with a folded towel placed between the thighs, under the scrotal sac (4). An institutional MR imaging protocol is provided in Table 1. The normal testes are homogeneous, isointense to muscle on T1-weighted images, and hyperintense on T2-weighted images. On T1- and T2-weighted images, the testes are encircled by a low-signal-intensity covering representing the tunica albuginea (Fig 2) (3). On T2-weighted images, the mediastinum testis is identified as a low-signal-intensity band within the posterior portion of the testis. Axial dual-echo (in-phase and opposed-phase) T1-weighted spoiled gradient-echo sequences are used to reveal intracellular lipid; these sequences are also helpful in identifying chronic hemorrhage, as hemosiderin is more conspicuous with gradient-echo sequences because of the T2* effect, which causes blooming with in-phase sequences because of progressive dephasing with the longer echo time (2,5). Fat-suppressed sequences should be used in cases where a fatty lesion is a consideration (6). The epididymis is slightly heterogeneous and hypo- to isointense relative to the testis on T1-weighted images and is hypointense on T2-weighted images. After contrast agent administration, the epididymis shows hyperenhancement relative to the testis (7). Diffusion-weighted imaging is useful for detection of malignant neoplasms and scrotal abscesses and is largely dependent on the extent of tissue cellularity, densely packed neoplastic cells, and enlargement of nuclei, all of which are associated with restricted diffusion owing to the reduced mobility of water molecules. The mean ADC values for normal testicular parenchyma are in the range of $1.08–1.31 \times 10^{-3}$ mm^2/sec, depending on patient age, and are lower in malignant lesions than in benign lesions or normal tissue (8,9). Axial T1-weighted imaging with an extended or large field of view is used to image the abdomen and pelvis when cryptorchidism or malignancy is suspected, to exclude metastasis (4).

Extratesticular Pathologic Conditions

Extratesticular Lipoma

Lipoma is the most common benign mesenchymal extratesticular tumor, comprising 45% of all extratesticular scrotal masses (10,11). Lipomas affect patients over a wide age range and are often discovered incidentally as nontender scrotal masses. At US, lipomas are typically well-defined hyperechoic lesions without internal flow at color Doppler US. Occasionally, an admixture of other mesenchymal elements, such as fibrous connective tissue or vascular tissue, alters the architecture of a lipoma (12). However, MR imaging can be helpful for definitive diagnosis. Lipomas have high signal intensity on both T1- and T2-weighted images and no contrast enhancement, which helps differentiate them from liposarcoma. High signal intensity on T1-weighted images can be noted with hemorrhagic lesions; therefore, fat-suppressed images are essential to confirm the diagnosis (Fig 3) (6,13). Management of lipomas is excision if the tumor is symptomatic or if a definitive diagnosis with imaging cannot be made (10).

Adenomatoid Tumor

Adenomatoid tumors are the second most common extratesticular tumor and the most common benign tumor of the epididymis and account for 30% of all extratesticular tumors (14). Adenomatoid

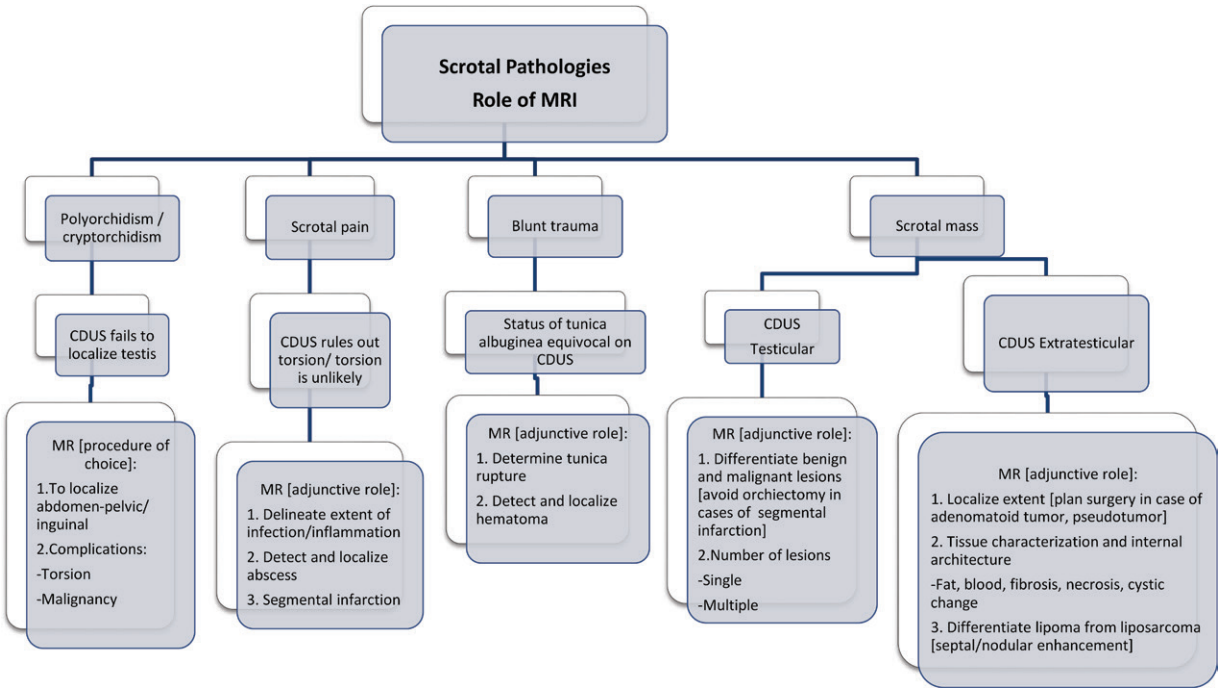

Figure 1. Role of MR imaging in the evaluation of scrotal pathologic conditions. *CDUS* = color Doppler US; *MR, MRI* = MR imaging.

Table 1: Institutional Protocol for 1.5-T MR Imaging of the Scrotum

Parameter	Sagittal T2W SSFSE	Axial T2W SSFSE	Axial T2W SSFSE SPAIR	Axial GRE (In, Opp)	Axial 3D T2W FSE	Axial T2W SSFP	Coronal 3D T1W FS GRE (Pre, Post)	Axial 3D T1W FS GRE Multi-phase	Axial T1W FS FSE SPAIR	Axial Pelvic DWI*
TR (msec)/ TE (msec)	1500/90	1500/89	1500/80	160/2.33, 4.99	1200/123	2.76/1.13	3.77/1.35	3.81/2.11	550/9.6	7300/76
FA (degrees)	180	180	180	70	150	80	10	10	150	90
FOV (mm)	256 × 256	380 × 323	380 × 323	380 × 309	256 × 256	360 × 293	400 × 367	380 × 317	250 × 250	300 × 300
Matrix	256 × 256	320 × 320	320 × 320	320 × 224	256 × 256	256 × 256	288 × 187	288 × 216	256 × 230	192 × 192
Thickness (mm)	5	6	6	6	1	6	3	3	4	5.5
NSA	1	1	1	1	1.4	1	1	1	2	10
No. of accel-erations	2	2	2	2	2	2	2	2	2	2
Time (min:sec)	0:53	0:53	0:53	0:29	5:40	0:14	0:18	0:18	5:26	2:04

Note.—DWI = diffusion-weighted imaging, FA = flip angle, FOV = field of view, FS = fat-suppressed, FSE = fast spin echo, GRE = gradient echo, In = in phase, NSA = number of signals acquired, Opp = opposed phase, Post = contrast-enhanced, Pre = nonenhanced, SPAIR = spectral attenuated inversion-recovery, SSFP = steady-state free precession, SSFSE = single-shot FSE, TE = echo time, 3D = three-dimensional, T1W = T1-weighted, T2W = T2-weighted, TR = repetition time.
*b = 0 sec/mm^2, b = 50 sec/mm^2, and b = 1000 sec/mm^2.

tumors are mesodermal in origin. Forty percent occur in the tail of the epididymis, but they can be found elsewhere, including in the tunica (14%), epididymal head (12%), and testis (7.5%) and in unspecified locations (25%) (15–17). Adenomatoid tumors can occur in the spermatic cord and tunica albuginea, where they can grow intratesticularly, mimicking germ cell tumors (14). These tumors occur at a wide range of ages, with the majority found in patients aged 20–25 years. Patients usually present with a painless scrotal mass. Adenomatoid tumors are smooth, round, well-circumscribed masses ranging in size from a few millimeters to 5 cm (6). At US, their appearance is variable, ranging from hyperechoic to hypoechoic to isoechoic relative to adjacent tissues. Differentiation from peripheral testicular parenchymal masses can be difficult at US; MR imaging may be helpful in distinguishing an extratesticular neoplasm from an intratesticular mass in the periphery of the testis

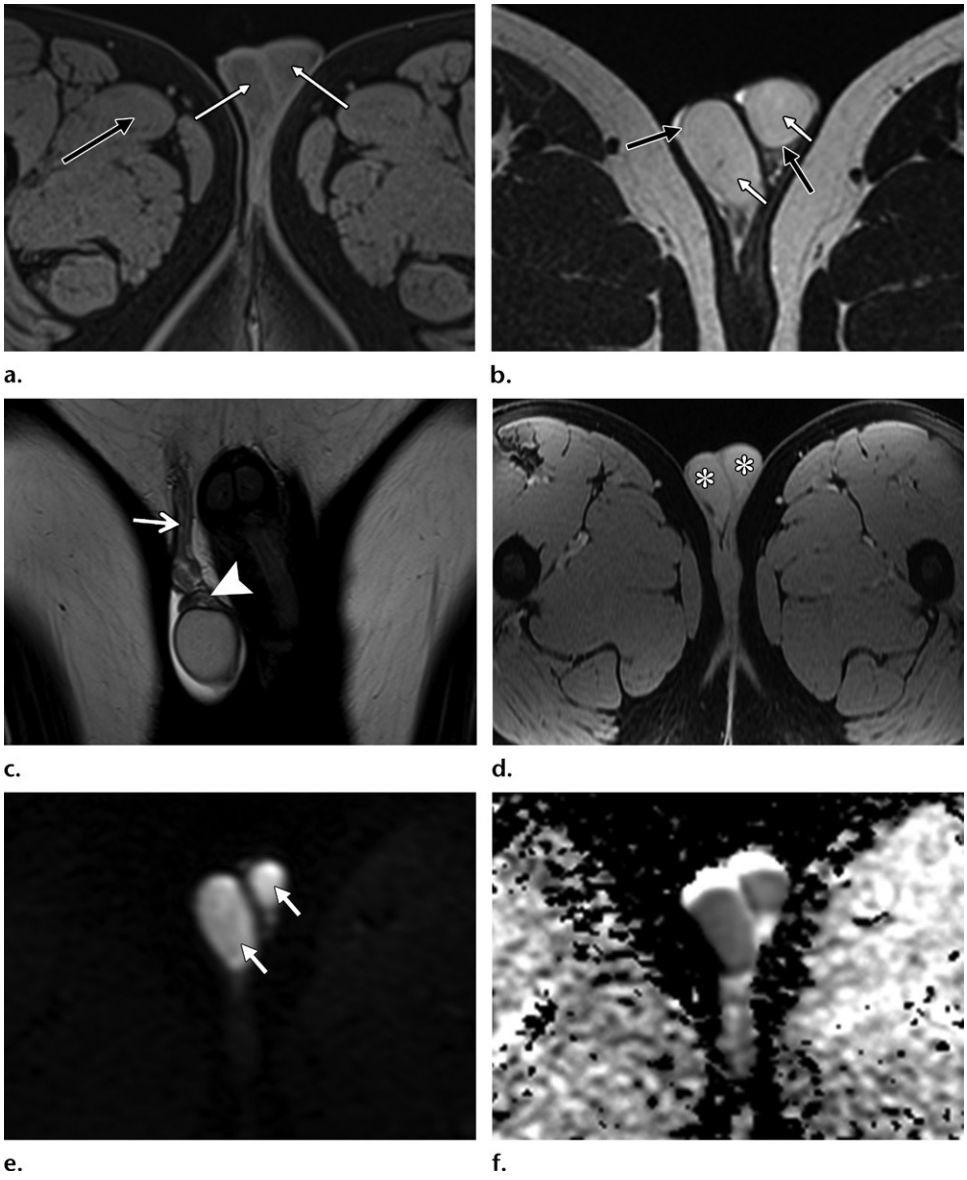

Figure 2. Normal testes in a 30-year-old man. **(a)** Axial T1-weighted MR image through the scrotum shows normal testes (white arrows) with signal intensity similar to that of the surrounding muscles (black arrow). **(b)** Axial T2-weighted MR image shows the hyperintense parenchyma of normal testes (white arrows) surrounded by a thin lining of hypointense tunica albuginea (black arrows). **(c)** Coronal T2-weighted MR image shows the normal right spermatic cord (arrow) and epididymal head (arrowhead), which are hypointense compared with the testis. **(d)** Axial contrast-enhanced T1-weighted MR image shows homogeneous enhancement of the testicular parenchyma (*). **(e)** Axial diffusion-weighted MR image (b = 800 sec/mm^2) depicts normal testicles with high signal intensity (arrows). **(f)** Apparent diffusion coefficient (ADC) image shows ADC values within normal limits (right testis, 1.10×10^{-3} mm^2/sec; left testis, 1.17×10^{-3} mm^2/sec).

(16). At T2-weighted MR imaging, adenomatoid tumors are hypointense relative to the testicular parenchyma. These tumors demonstrate slow or decreased contrast enhancement relative to the testicular parenchyma or contralateral testis. However, the enhancement can be variable because, less commonly, adenomatoid tumors show hyperenhancement relative to the testis (Fig 4) (16,18). Management of extratesticular adenomatoid tumors involves intraoperative frozen section biopsy used to confirm the diagnosis and local excision, whereas intratesticular adenomatoid tumors are treated with testicular-sparing surgery (10).

Fibrous Pseudotumor

Fibrous pseudotumor is an uncommon extratesticular lesion with an incompletely understood etiology. It is not considered a true neoplasm but a benign reactive proliferation of inflammatory and fibrous tissue involving the tunica, in response to trauma, surgery, infection, or inflammation (15,19,20). A rare association has been reported with *Schistosoma haematobium* and human immunodeficiency virus (HIV) infection (19). About 50% of cases have an associated hydrocele, while 30% of cases are associated with prior trauma or epididymo-orchitis (2,19). The most common occurrence of fibrous tumors is in the 3rd decade of life; they are rare before 18 years of age (21). Patients typically present with a painless scrotal lump of widely varying size or with unilateral scrotal swelling (21). At histologic analysis, a fibrous pseudotumor is composed of dense fibrous tissue with interspersed fibroblasts mixed with inflammatory cells; it has been classified into several forms: *(a)* The nodular type is the most common type and appears as a fibrous nodule or

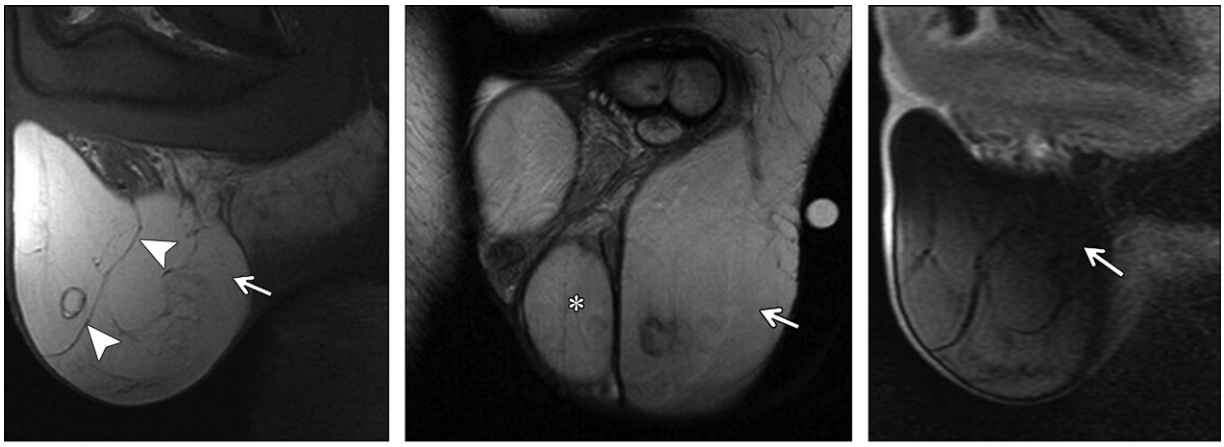

Figure 3. Extratesticular lipoma in a 40-year-old man. **(a, b)** Sagittal T1-weighted **(a)** and coronal T2-weighted **(b)** MR images show a moderately large well-encapsulated hyperintense mass (arrow) in the left hemiscrotum that displaces the left testis (* in **b**) medially. Fine hypointense septa are noted within the mass (arrowheads in **a**). **(c)** Sagittal contrast-enhanced fat-suppressed T1-weighted MR image shows suppression of internal signal intensity (arrow) in the lesion, a finding compatible with fat content. No enhancement of the septa and no enhancing solid nodule are noted within the lesion, findings that help differentiate the lesion from a more aggressive liposarcoma.

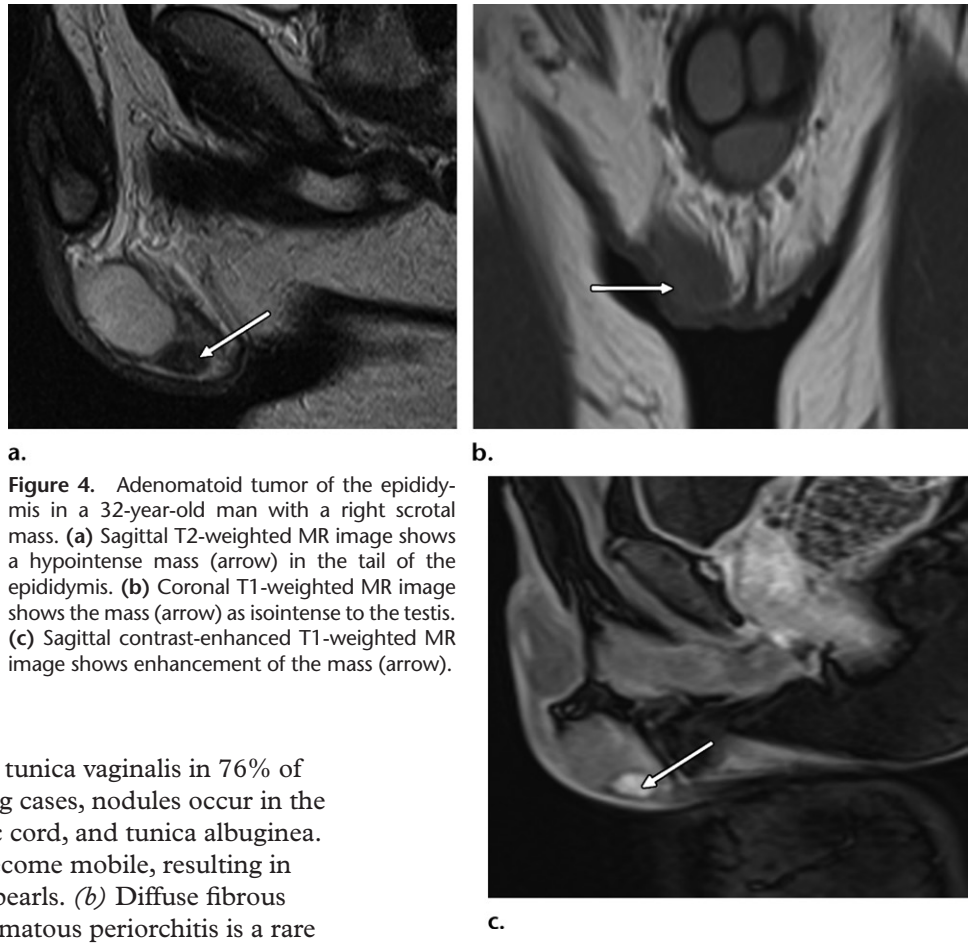

Figure 4. Adenomatoid tumor of the epididymis in a 32-year-old man with a right scrotal mass. **(a)** Sagittal T2-weighted MR image shows a hypointense mass (arrow) in the tail of the epididymis. **(b)** Coronal T1-weighted MR image shows the mass (arrow) as isointense to the testis. **(c)** Sagittal contrast-enhanced T1-weighted MR image shows enhancement of the mass (arrow).

nodules arising in the tunica vaginalis in 76% of cases; in the remaining cases, nodules occur in the epididymis, spermatic cord, and tunica albuginea. These nodules can become mobile, resulting in scrotoliths or scrotal pearls. *(b)* Diffuse fibrous pseudotumor or fibromatous periorchitis is a rare form that may partly or completely encase the testis. *(c)* Inflammatory fibrous pseudotumor most commonly involves the spermatic cord and rarely extends to the testis (15,19). The nodular type of fibrous pseudotumor may be treated with excision of the tunica vaginalis, whereas the diffuse form is treated with orchiectomy (15). The US appearance of fibrous pseudotumor is widely variable depending on the fibrous and cellular components and may be associated with acoustic shadowing when calcifications are present in the mass (6). It is important that fibrous pseudotumor of the

Figure 5. Fibrous pseudotumor in a 30-year-old man. **(a)** Sagittal T2-weighted MR image shows a well-circumscribed hypointense lesion in the right hemiscrotum (arrow) posterior to the right testis (*). **(b, c)** Axial early phase **(b)** and sagittal delayed phase **(c)** contrast-enhanced fat-suppressed T1-weighted MR images show gradual and persistent enhancement of the lesion (arrow).

scrotum not be mistaken for malignancy, as treatment of fibrous pseudotumor is most commonly local excision rather than orchiectomy.

MR imaging is useful for more definitive preoperative diagnosis and helps guide surgical management. At MR imaging, the tumor demonstrates intermediate to low signal intensity on T1-weighted images and low signal intensity on T2-weighted images secondary to fibrous tissue. The tumor demonstrates slow but persistent contrast enhancement, which can be variable but is characteristic of fibrous tissue (Fig 5) (2,22).

Extratesticular Hematoma

Extratesticular hematomas within the tunica vaginalis and scrotal wall are most commonly seen after blunt trauma. As is true for hematomas in other locations, the US appearance of extratesticular hematoma varies with the age of the hematoma; acute hematomas are echogenic, whereas chronic hematomas become anechoic over time, may develop septa and lobulations, and may show fluid-fluid levels along with echoes indicative of clots (15,23). The MR imaging features also depend on the degeneration of the hematoma. Hematomas are usually hyperintense on T1-weighted images because of intracellular and extracellular methemoglobin but show variable signal intensity on T2-weighted images. A dark hemosiderin ring on T2-weighted images signifies chronicity. No enhancement is seen after contrast material administration (Fig 6) (18). Acute hematomas may mimic testicular torsion owing to reduced blood flow to the testis because of extrinsic pressure on the vessels (23). Evacuation of an extratesticular hematoma may result in restoration of normal testicular blood flow. Extratesticular hematomas may be iatrogenic, occurring as a complication of orchiectomy or inguinal herniorrhaphy (24).

Tuberculous Epididymo-orchitis

Chronic epididymitis is most frequently noted in granulomatous conditions such as tuberculosis, brucellosis, syphilis, and fungal infections. Genitourinary tuberculosis is the most common manifestation of extrapulmonary tuberculosis caused by *Mycobacterium tuberculosis*. The scrotal contents are usually involved by retrograde extension from the prostate and seminal vesicles, although hematogenous dissemination has also been suggested (25). Tuberculosis of the scrotum is rare and occurs in about 7% of patients with tuberculosis (26). The disease usually starts in the tail of the epididymis, either because of its rich blood supply or because it is the first portion involved by urinary reflux; the vas deferens may also be involved. The disease may propagate to the entire epididymis, finally involving the testis (27). Isolated involvement of the testis is rare (26). At US, the testis appears markedly heterogeneous, which is explained by a variety of pathologic components such as caseation necrosis, fibrosis, and granulation. Lesions become more heterogeneous as calcifications and sinuses draining necrotic pus form. Sinus or fistulous tracts in tuberculosis occur as a result of a caseous abscess reaching the skin; a chronic draining sinus tract should be considered of tuberculous origin unless proven otherwise (27). At US, several patterns of tuberculous epididymo-orchitis have been described:

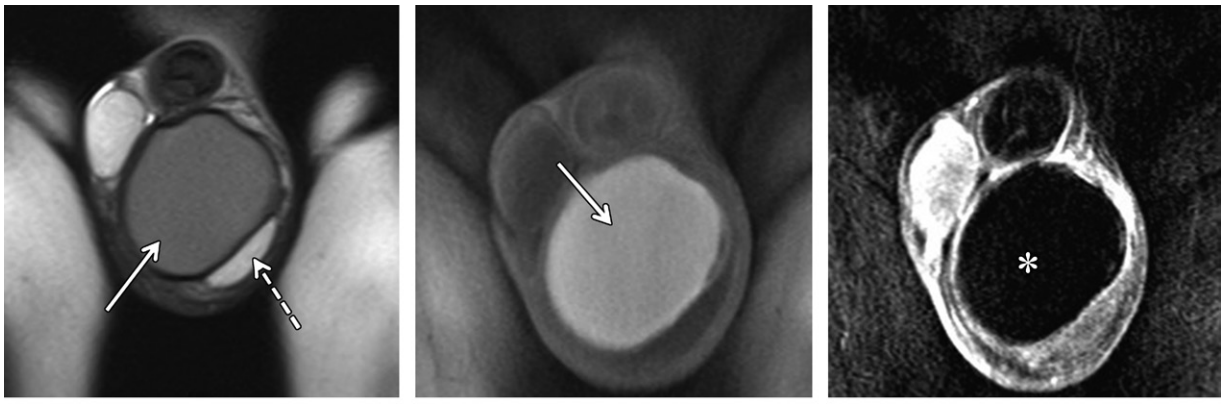

a. b. c.

Figure 6. Chronic organized extratesticular hematoma in a 31-year-old man who presented with asymmetric hard left testicular swelling of 2 months' duration. Tumor markers were normal. **(a)** Coronal T2-weighted MR image of the scrotum shows a well-encapsulated T2-intermediate lesion (solid arrow) with a hypointense ring due to hemosiderin and a normal-appearing left testis (dashed arrow) that is compressed and displaced, findings which helped confirm the extratesticular location of the hematoma. **(b, c)** Coronal T1-weighted **(b)** and contrast-enhanced subtraction **(c)** MR images show that the lesion is hyperintense (arrow in **b**) with no contrast enhancement (∗ in **c**).

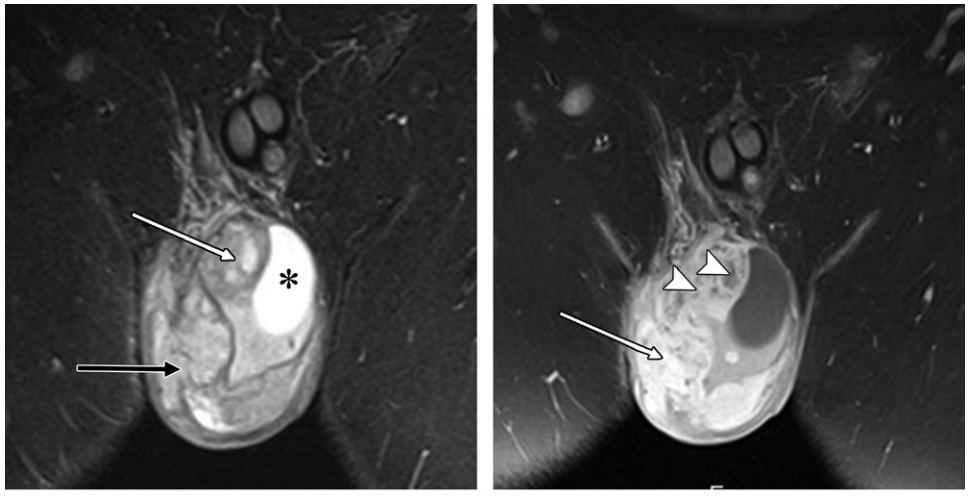

a. b.

Figure 7. Tuberculous epididymo-orchitis in a 27-year-old man with scrotal pain and swelling. **(a)** Coronal fat-suppressed T2-weighted MR image through the scrotum shows a diffusely thickened epididymis and a heterogeneous right testis, which is displaced (white arrow); a hydrocele (∗); and thickened overlying subcutaneous tissues and a discontinuous tunica vaginalis (black arrow). **(b)** Coronal contrast-enhanced T1-weighted MR image shows diffuse heterogeneous enhancement of the thickened epididymis and testis (arrow). Multiple tiny nonenhancing areas (arrowheads) within the epididymis and testis have high T2 signal intensity on **a**, findings consistent with microabscesses.

(a) a diffusely enlarged heterogeneous hypoechoic epididymis and/or testis, *(b)* a diffusely enlarged homogeneous hypoechoic epididymis and/or testis, *(c)* nodular enlargement and a heterogeneous hypoechoic epididymis and/or testis, and *(d)* multiple small hypoechoic nodules in the enlarged testis (26,27). At MR imaging, the tuberculous lesion shows low signal intensity on T2-weighted images, a finding attributed to chronic inflammation, fibrosis, and calcifications, because tuberculosis of the scrotum is usually diagnosed at a chronic stage. Signal intensity on T1-weighted images is variable, and areas of high signal intensity can be demonstrated. Contrast enhancement of the lesion is also variable, ranging from no enhancement to strong enhancement (Fig 7) (25). The differential diagnosis includes bacterial epididymo-orchitis and tumor. A clinical history of tuberculosis, presence of lymphadenopathy, absence of tumor markers, increased temperature of the scrotum, and response failure to conventional antibiotic therapy are suggestive of tuberculous epididymo-orchitis. Antituberculosis chemotherapy is the initial treatment of tuberculosis, but in certain cases, it is difficult to differentiate a tuberculous lesion from tumorlike conditions, especially when the lesion does not respond to antituberculous treatment. In those cases, surgical exploration is required (15).

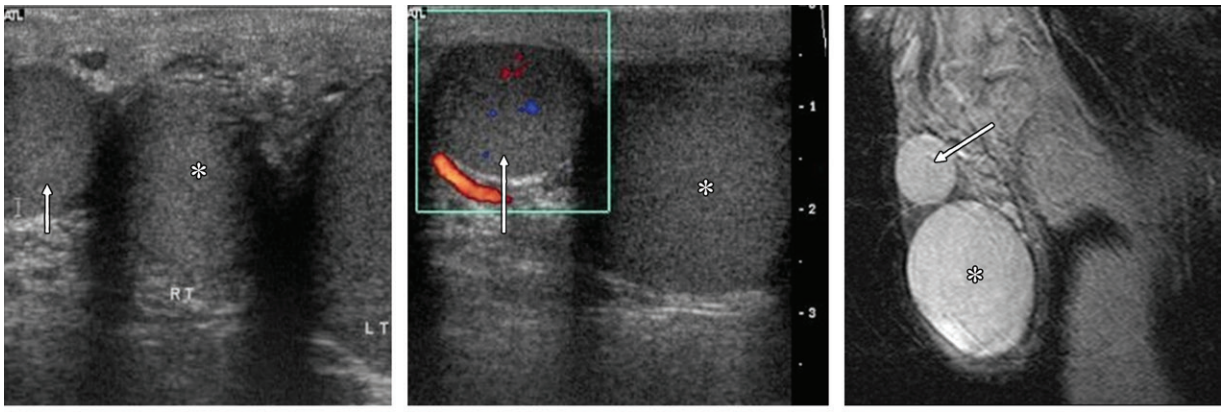

Figure 8. Polyorchidism in a 21-year-old man. **(a, b)** Longitudinal gray-scale **(a)** and transverse color Doppler **(b)** US images of the scrotum show a well-defined rounded mass (arrow) superior and lateral to the right testis (*RT;* ∗). The mass is similar in echogenicity to the testis and shows internal vascularity. *LT* = left testis. **(c)** Sagittal T2-weighted MR image shows a supernumerary testis (arrow) as a well-defined mass superior and similar in signal intensity to the right testis (∗).

Polyorchidism

Polyorchidism is defined as the presence of more than two testes, a rare developmental anomaly that occurs as a result of longitudinal or transverse division of the genital ridge by the development of peritoneal bands (28). Triorchidism is the most common type. Bilateral supernumerary testes have also been reported. In approximately 75% of cases, the supernumerary testes are intrascrotal and superior or inferior to the ipsilateral testes; 20% are inguinal, and the remaining 5% are retroperitoneal (6). Approximately 4% of cases of polyorchidism occur in association with cryptorchidism, and 15% are associated with testicular torsion owing to mobility (28). Most cases of polyorchidism are discovered in young males (mean age, 15–20 years) (28). Polyorchidism is usually incidental and manifests as a painless mass. On the basis of anatomy and function, polyorchidism is classified into two types: *(a)* reproductively functional, where the supernumerary testis is drained by a vas deferens; and *(b)* reproductively nonfunctional, with an undrained supernumerary testis (29). Malignant transformation within the supernumerary testis may occur regardless of its location. The most common neoplasms are germ cell tumors, such as embryonal carcinoma and seminoma (28). Spermatogenesis is normal in about 50% of cases; however, reduced or abnormal spermatogenesis has also been reported (28). At US, the echo and flow patterns of the supernumerary testis are identical to those of the normal testis. In cases that are equivocal at US, MR imaging is extremely useful for definitive diagnosis. MR imaging reveals a round or oval mass with homogeneous intermediate signal intensity on T1-weighted images and high signal intensity on T2-weighted images, findings that are typical for normal testicular tissue (Fig 8). Contrast enhancement is also similar to that of normal testes (2,28). Management of polyorchidism is controversial, as there are no clear guidelines; most cases are managed conservatively if the clinical and imaging findings demonstrate no complications. However, in cases of cryptorchidism, torsion, or malignancy, surgical removal is suggested (2,28,30). MR imaging plays a confirmatory role and may provide additional information in conditions that may complicate polyorchidism, such as cryptorchidism or neoplasms (28).

Sclerosing Lipogranuloma

Sclerosing lipogranuloma is a benign condition of unclear pathogenesis, but it is known to be an inflammatory response to endogenous fatty degeneration occurring in the subcutaneous tissues of the scrotum and dorsal aspect of the penis. It was first described by Smetana and Bernhardt in 1950 (31,32). A majority of cases are secondary to injection of foreign bodies such as liquid paraffin, mineral oil, or silicone, but in a subset of cases there is no foreign body injection (10,32,33). There are two types of sclerosing lipogranuloma: *(a)* primary, caused by the breakdown of endogenous lipids; and *(b)* secondary, caused by injection of an exogenous foreign body (32). The condition usually manifests as a symmetrical *Y*-shaped hard granuloma involving the scrotum or penoscrotal junction (69% of cases) (34). In 24% of cases, the findings are asymmetric (35). Definitive diagnosis is made at histologic analysis. The cut surface of the rubbery mass is a solid whitish-yellow color. Microscopically, vacuoles of variable sizes correspond to the exogenous substance surrounded by sclerotic or collagenous stroma (10,32). Because it is a granulomatous lesion, it contains epithelioid cells, multinucleated giant cells, fibroblasts, lymphocytes, eosinophils, and macrophages (31). At T1- and T2-weighted MR imaging, it demonstrates heterogeneous signal intensity and

Figure 9. Sclerosing lipogranuloma in a 40-year-old man after silicone injection into the penoscrotal region for penile enhancement. **(a, b)** Sagittal T1-weighted **(a)** and fat-suppressed T1-weighted **(b)** MR images show an ill-defined masslike lesion with heterogeneous signal intensity in the left hemiscrotum, with focal areas of signal dropout (arrow in **b**) suggestive of fat content (lipid vacuole). **(c)** Axial gadolinium-enhanced fat-suppressed T1-weighted MR image shows focal areas of heterogeneous contrast enhancement (arrow) in the lesion.

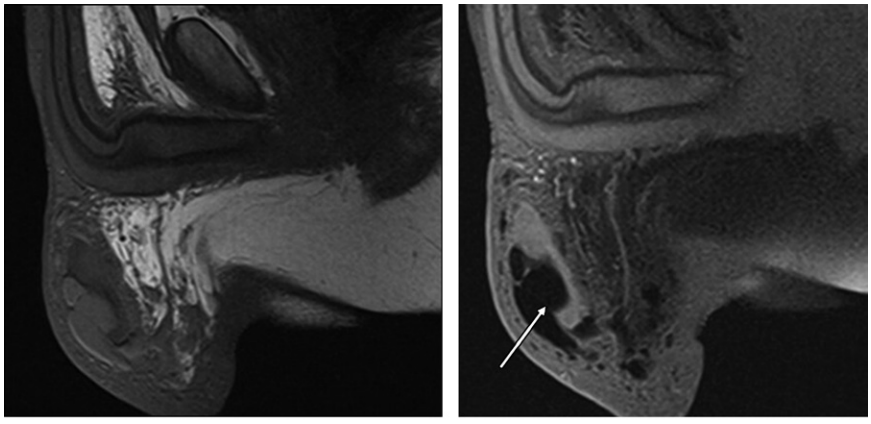

a. **b.**

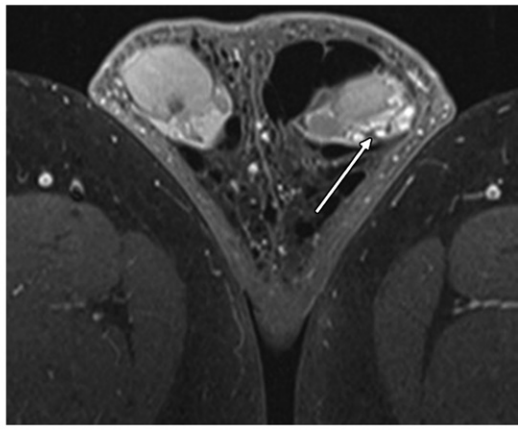

c.

heterogeneous contrast enhancement. It can be mildly hyperintense on T1-weighted images and hypointense on T2-weighted images owing to fibrous tissue. Small areas of T2 hyperintensity without enhancement in the lesion suggest cystic or necrotic changes (Fig 9) (32). Tuberculosis and fungal infections should be considered in the differential diagnosis for sclerosing lipogranuloma. Necrotic material may be seen in these conditions; multinucleated giant cells with fat vacuoles are diagnostic for sclerosing lipogranuloma (31). Steroid therapy has been recommended as a first-line treatment, but biopsy and surgical excision are frequently preferred in the treatment of sclerosing lipogranuloma (34).

Spermatic Cord/Paratesticular Liposarcoma

Liposarcomas are a group of malignant tumors of adipose tissue that arise from mesenchymal cells. Liposarcomas are located in the extremities or the retroperitoneum in 70% of cases. Paratesticular liposarcomas are rare, accounting for 7%–10% of all intrascrotal tumors (36,37). In adults, more than 75% of these lesions occur in the spermatic cord (37). Liposarcoma usually manifests as a nontender slow-growing mass in the scrotum or inguinal region. The mean age at presentation is 56 years, although a range of 16–90 years has been reported (6,38). Spermatic cord liposarcomas often can be mistaken for uncomplicated or incarcerated inguinal hernias, hydroceles, spermatoceles, hematoceles, or benign or malignant tumors of the testis and epididymis (eg, lipoma, leiomyoma, and rhabdomyosarcoma). The World Health Organization (WHO) classifies soft-tissue sarcomas into five categories, with increasing malignancy grades: well differentiated, dedifferentiated, myxoid, round cell, and pleomorphic. Well-differentiated liposarcomas are further subdivided into adipocytic (lipoma)–like and sclerosing types (39). Most liposarcomas of the spermatic cord are well-differentiated low-grade malignancies with no or minimal tendency to metastasize, but they can be locally invasive (40). Liposarcomas are immunoreactive for MDM2 and CDK4 markers, which helps to differentiate these tumors from lipomas. However, the most specific marker is S-100 protein, which is positive in 90% of cases (36). At US, liposarcomas are predominantly hyperechoic owing to their predominate fat composition but have variable echogenicity because of variable amounts of internal soft-tissue septa and calcifications (2). At MR imaging, macroscopic fat can be identified as regions of increased T1 and T2 signal intensity, with signal loss on fat-suppressed images. In addition, chemical shift artifact can be seen at the junction of soft-tissue and fat components within the tumor. The tumor shows heterogeneous contrast enhancement (Fig 10) (22).

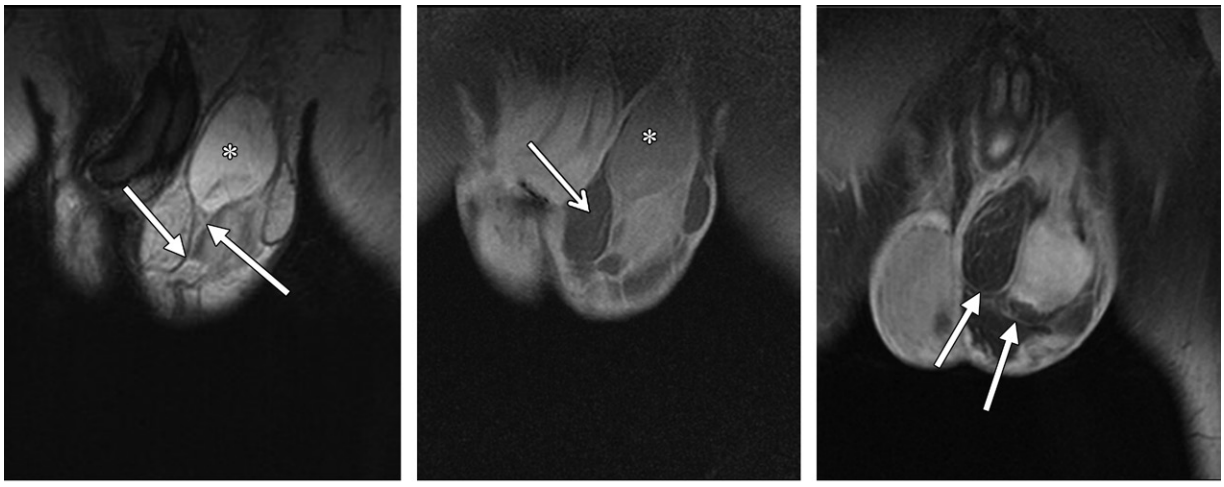

a. b. c.

Figure 10. Scrotal liposarcoma in a 60-year-old man. **(a, b)** Coronal T2-weighted **(a)** and fat-suppressed T1-weighted **(b)** MR images show a poorly circumscribed mass with internal fat content (arrow in **b**) and hypointense septa (arrows in **a**) in the left hemiscrotum encasing the left testis (*). **(c)** Coronal contrast-enhanced fat-suppressed T1-weighted MR image shows enhancement of the internal septa (arrows).

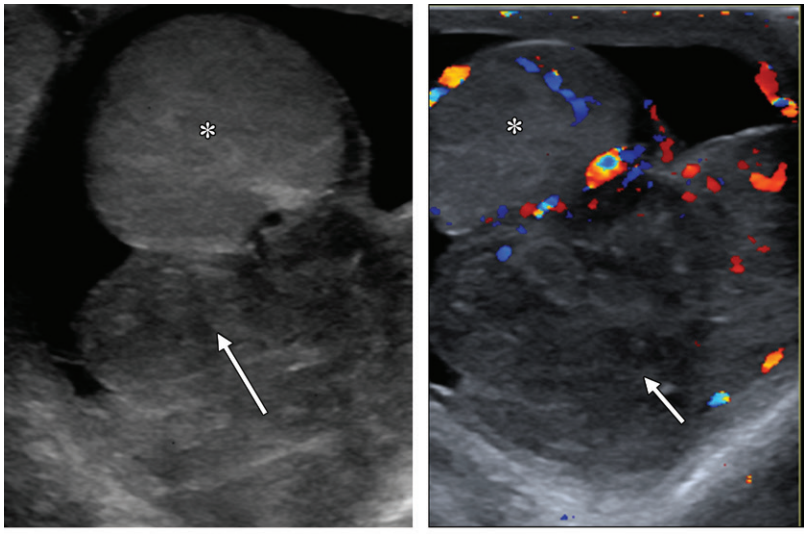

a. b.

Figure 11. Rhabdomyosarcoma in a 19-year-old man with left-sided scrotal swelling. Transverse gray-scale **(a)** and color Doppler **(b)** US images of the scrotum demonstrate a large heterogeneous left paratesticular mass (arrow) extending to the left testis (*), which shows internal vascularity. The left testis is otherwise unremarkable. The biopsy results were consistent with a diagnosis of rhabdomyosarcoma.

Liposarcoma is the most radiosensitive sarcoma. For intermediate- or high-grade tumors, treatment includes radical orchiectomy and adjuvant radiation with or without chemotherapy. In 40% of cases, positive lymph nodes can be identified (10).

Rhabdomyosarcoma

Rhabdomyosarcomas are rare tumors that occur mainly in the first 2 decades of life, with the median age at diagnosis being 7 years of age. Seven percent of rhabdomyosarcomas involve the paratesticular tissues (41). Histogenesis is related to the embryonic development of the spermatic cord, epididymis, testis, and connective tissue coverings (42). Pleomorphic, alveolar, and embryonal are the three histologic subtypes of rhabdomyosarcomas; the embryonal subtype is the most common, and the alveolar subtype has the worst prognosis (10,36). Rhabdomyosarcomas manifest as firm masses that may envelope or invade the epididymis and testis (Fig 11) (6). The US and MR imaging findings are nonspecific. Rhabdomyosarcomas have variable echogenicity, and color Doppler US shows increased vascularity and a low resistive index (43). A hydrocele may also be present (15).

Testicular Nonmalignant Pathologic Conditions

Testicular Ectasia of the Rete Testis

Dilated rete testis, or tubular ectasia of the rete testis, is a benign condition of the testis resulting from partial or complete occlusion of the efferent

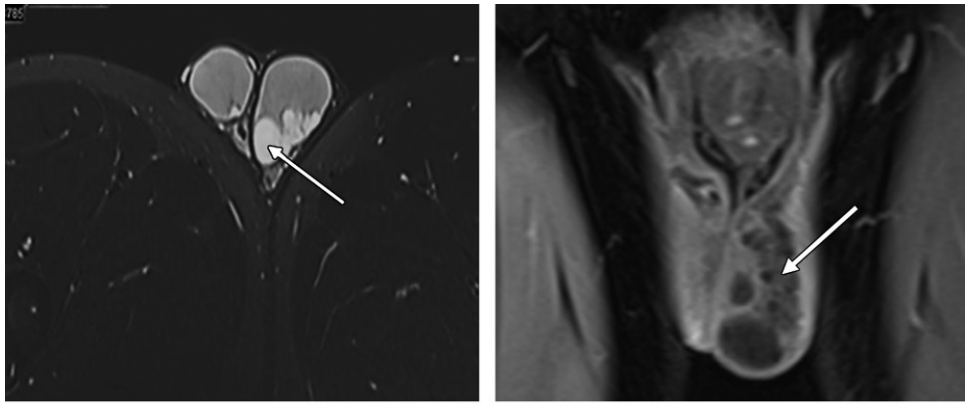

a. b.

Figure 12. Tubular ectasia of the rete testis in a 36-year-old man. **(a)** Axial T2-weighted MR image through the scrotum shows hyperintense cystic tubular structures in the region of the left mediastinum testis (arrow). **(b)** Coronal contrast-enhanced T1-weighted MR image reveals no enhancement (arrow).

Figure 13. Testicular abscess in a 60-year-old man who presented with fever and scrotal swelling. **(a)** Sagittal T2-weighted MR image demonstrates areas of hyperintensity (arrows) and a hypointense rim (arrowhead) involving the left testis. **(b)** Corresponding axial contrast-enhanced T1-weighted MR image through the scrotum shows no internal enhancement (*) but shows enhancing septa (black arrow) and enhancement of the surrounding parenchyma (white arrows).

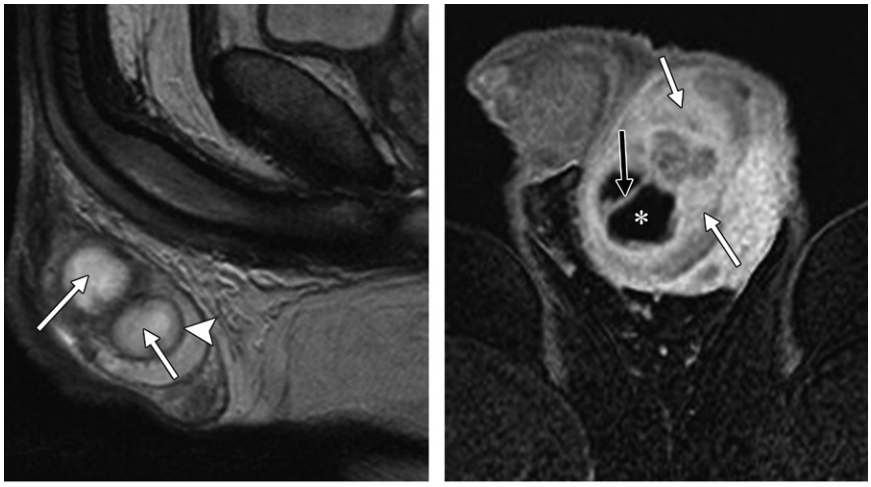

a. b.

ductules (44). It is often bilateral and associated with ipsilateral spermatoceles or epididymal cysts (21). It is more common in men older than 50 years and is recognized by its typical location in or around the mediastinum testis (18,44,45). At US, it appears as multiple cystic or tubular anechoic structures located in or adjacent to the mediastinum testis. The lack of mass effect or internal flow and the degree of complexity are helpful to distinguish tubular ectasia of the rete testis from an intratesticular varicocele or cystic neoplasms such as cystadenoma (18,44). At T2-weighted MR imaging, cystic dilatation of the rete testis appears hyperintense and shows no contrast enhancement (Fig 12) (18).

Testicular Abscess

Testicular abscesses are usually a result of inadequately treated bacterial epididymo-orchitis, occasionally after trauma, infarction, or mumps. They are less commonly caused by tuberculosis (5,46). Testicular abscesses are seen at US as focal intratesticular hypoechoic lesions with peripheral but no internal vascular flow, ill-defined shaggy walls, and low-level internal echoes caused by debris (47). The surrounding testicular parenchyma may be hypervascular (2). At MR imaging, the abscess manifests as a T2-hyperintense fluid collection with variable T1 signal intensity and peripheral enhancement and testicular parenchymal enhancement. The lesion also demonstrates signal hyperintensity on diffusion-weighted images, with corresponding low signal intensity on ADC maps, findings indicative of restrictive diffusion (Fig 13) (5). Sometimes it is difficult to differentiate testicular torsion and hematoma from abscess because all three entities will show absent or decreased blood flow; in cases of torsion, there will be no hypervascularity of the epididymis, which is typically present with infection. In cases of hematoma, there typically is antecedent trauma, and follow-up MR imaging will demonstrate degrading blood products (5,46).

a. b.

Figure 14. Testicular trauma with an intact tunica albuginea in a 34-year-old man. **(a)** Coronal T2-weighted MR image of the scrotum shows abnormal areas of low signal intensity involving the left testis (arrowhead), with integrity of the low-signal-intensity line that represents the tunica albuginea (arrows). **(b)** Corresponding axial nonenhanced T1-weighted MR image shows areas of high signal intensity (arrow) due to hemorrhage.

Testicular Trauma

Blunt scrotal trauma may cause contusion, hematoma, fracture, or rupture. Depending on the age of the hematoma, the US appearance can be variable, as acute testicular hematomas are hyperechoic and simulate a focal mass. After 1–2 weeks, hematomas undergo liquefaction and may appear cystic (18). At MR imaging, in the subacute stage, both intracellular methemoglobin and extracellular methemoglobin are hyperintense on T1-weighted images but show variable signal intensity on T2-weighted images. Low signal intensity is seen on T2-weighted images in chronic hematoma, secondary to hemosiderin deposition within the macrophages. No contrast enhancement is seen (18). Serial follow-up imaging of traumatic testicular lesions should be performed because up to 15% of tumors can be detected after episodes of trauma. Traumatic lesions tend to resolve, whereas tumors continue to grow (47).

US has high sensitivity for depicting testicular injuries as a focal area of altered testicular echogenicity that corresponds to contusion, infarction, hematoma formation, discrete fracture, and irregularity of the tunica albuginea (23,48,49). At MR imaging, the normal testis has homogeneous intermediate T1 signal intensity and high T2 signal intensity and is surrounded by a fibrous layer of tunica albuginea, which has low T1 and T2 signal intensity. In the context of a hematoma, areas of heterogeneous low T2 signal intensity raise the possibility of testicular injury, and interruption of the low-signal-intensity line representing the tunica albuginea is the key finding of testicular rupture; therefore, it is important to evaluate the tunica albuginea in all three imaging planes (Figs 14, 15) (48).

Segmental Testicular Infarction from Testicular Torsion

Segmental testicular infarction is an uncommon condition affecting part of a testis and is often diagnosed after partial or total orchiectomy (50). Global testicular infarction is a feature of spermatic cord torsion affecting adolescent boys 12–18 years of age (48,51). Testicular torsion is considered a true surgical emergency because the severity of ischemia and the viability of the testis are directly related to the duration and degree of torsion. The degree of torsion ranges from 180° to 720°. Venous obstruction occurs first, followed by arterial obstruction, which ultimately leads to testicular ischemia. Torsion of at least 540° is required for complete arterial occlusion (52,53). The salvage rate for the affected testis is nearly 100% if surgery is performed within 6 hours of the onset of torsion, it is 70% if surgery is performed within the first 6–12 hours, and it decreases to 20% if surgery is delayed more than 12 hours (54). Segmental infarction due to torsion is usually caused by torsion and detorsion of the testis producing ischemia of the testis, mostly commonly in the superior aspect of the testis because of a significant lack of collaterals in this region and secondary hyperemia of the lower pole (47,51). Imaging findings vary with the duration of torsion. In the acute phase, the testis may appear normal, but as ischemia progresses, the testis becomes heterogeneous, enlarged, and hyperemic. Further ischemia causes hypoechogenicity, a finding indicative of nonviability. Testicular hypoechogenicity and enlargement increase in the first 5 days and then decrease over the next 4–5 days (48,54). Testicular torsion can be treated by detorsion and orchiopexy if intraoperative Doppler US shows restoration of blood flow after detorsion. However, if the testis is

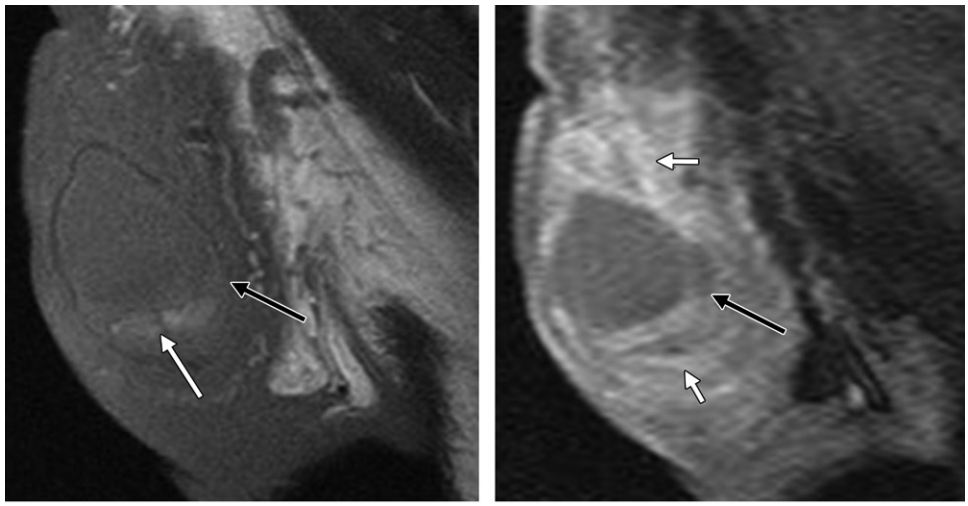

a. b.

Figure 15. Scrotal trauma with rupture of the tunica albuginea in a 34-year-old man. **(a)** Sagittal nonenhanced T1-weighted MR image shows a linear area of T1 signal hyperintensity at the junction of the middle and lower thirds of the left testis, suggestive of a fracture line, with a hematoma (white arrow). Black arrow = area of rupture of the tunica albuginea. **(b)** Sagittal contrast-enhanced T1-weighted MR image shows the area of the tunica albuginea rupture (black arrow) and enhancement of paratesticular tissue (white arrows).

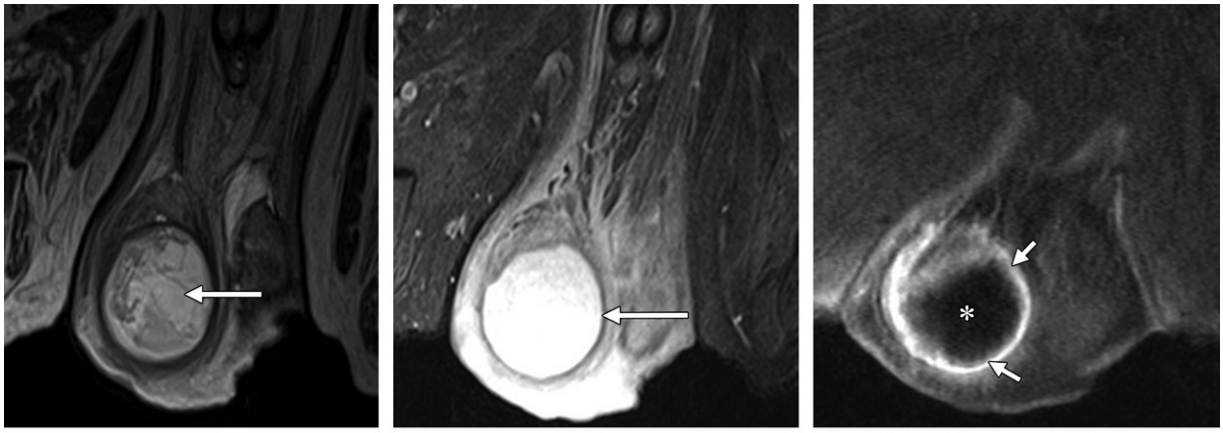

a. b. c.

Figure 16. Missed torsion and testicular infarction in a 35-year-old man who presented with acute right testicular pain. The patient had experienced similar pain a few months earlier for a short period of time, which was relieved without any medical intervention. **(a)** Coronal T2-weighted MR image demonstrates an area of heterogeneous signal intensity in the right testis (arrow). **(b)** Corresponding coronal contrast-enhanced T1-weighted MR image shows hyperintense signal (arrow) due to hemorrhage. **(c)** Coronal contrast-enhanced subtraction MR image shows no enhancement in the area (*). The peripheral rim of enhancement is due to vascularity from capsular enhancement (arrows).

irreversibly damaged, orchiectomy is preferred to prevent the development of antisperm antibodies. Segmental infarction at US is sometimes difficult to differentiate from testicular malignancy, but a complete absence of blood flow within the masslike area at color Doppler US should indicate infarction. MR imaging findings are supportive and confirmatory. A nonsalvageable testis develops segmental or complete hemorrhagic necrosis, with heterogeneous signal intensity on T2-weighted images and hyperintense signal on T1-weighted images. There is a lack of central contrast enhancement, with enhancement at the periphery of the testis (Fig 16) (2,55).

Segmental Testicular Infarction from Epididymo-orchitis

Segmental testicular infarction occurs in older patients with a median age of 40 years, which overlaps with the population that develops testicular tumors (51). Acute epididymo-orchitis is the most common cause of segmental infarction; other etiologic factors include sickle cell disease, polycythemia, hypersensitivity angiitis, testicular artery intimal fibromuscular dysplasia, and previous surgery (50). Segmental infarction is often indistinguishable from testicular malignancy. A complete absence of flow in a masslike area at color Doppler US is indicative

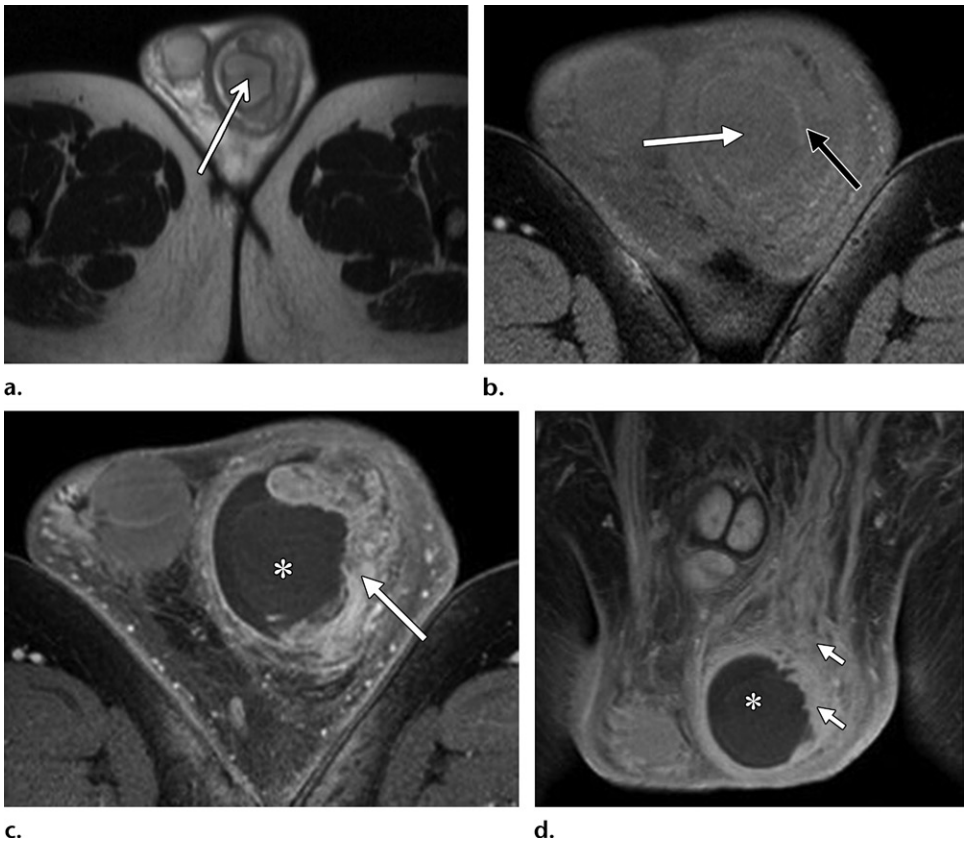

Figure 17. Segmental testicular infarction after an episode of epididymo-orchitis in a 48-year-old man who presented with acute left testicular pain. **(a)** Axial T2-weighted MR image shows an area of heterogeneous low signal intensity in the left testis (arrow). **(b)** Axial nonenhanced T1-weighted MR image through the scrotum shows a corresponding area that is isointense to the testis (white arrow), with hyperintensity along the periphery owing to hemorrhage (black arrow). **(c, d)** Axial **(c)** and coronal **(d)** contrast-enhanced T1-weighted MR images show rim enhancement (arrow in **c**) in the region of the infarcted testis (*), with enhancement of the viable testis and epididymis (arrows in **d**).

of infarction in the appropriate clinical setting (51). Untreated epididymitis may progress to involve the testis, spermatic cord, and prostate and lead to segmental testicular infarction owing to the following mechanisms: *(a)* venous outflow obstruction due to edema of the epididymis, especially the globus major, compressing the testis; *(b)* irreversible lymphatic, venous, and arterial occlusion of the spermatic cord due to inflammation (funiculitis); *(c)* endothelial damage and vascular thrombosis due to bacterial toxins; and *(d)* vascular compression at the external inguinal ring due to edema (50). Potential warning signs of ischemia include *(a)* acute worsening of pain despite initial clinical improvement, *(b)* nonresolving infection despite appropriate antibiotic therapy, *(c)* spermatic cord thickening and tenderness, *(d)* recurrent epididymo-orchitis, and *(e)* repeated febrile episodes despite suitable antibiotic therapy (56). At US, segmental infarction is observed as a solitary wedge-shaped or round area of heterogeneous or decreased echogenicity in either testis, with no particular anatomic predilection, associated with markedly diminished or absent vascular flow at color Doppler US, with the apex pointing toward the testicular mediastinum (57). At T2-weighted MR imaging, segmental infarction demonstrates variable signal intensity; the area of infarction may be hyperintense or hypointense compared to the normal testis but has well-defined low-signal-intensity borders. On T1-weighted images, the lesion is isointense, but sometimes high-signal-intensity foci can be seen owing to hemorrhage. Segmental infarction has reduced or no contrast enhancement. A rim of subcapsular enhancement can be present because of preserved parenchyma supplied by the cremasteric artery (Fig 17). In chronic disease, retraction of the tunica albuginea can be present in the area of infarction owing to volume loss and fibrosis (2,47,51). Diagnosis of segmental infarction remains challenging, and in many cases definitive diagnosis is made after orchiectomy. Acute testicular pain, normal tumor and inflammatory markers, and reduced or no contrast enhancement at MR imaging should prompt the diagnosis of segmental infarction, and unnecessary orchiectomy can be avoided (58,59).

Figure 18. Adrenal rest tumor in a 50-year-old man with known congenital adrenal hyperplasia. **(a, b)** Coronal T2-weighted **(a)** and sagittal T1-weighted **(b)** MR images show a mass (arrow) that is hypointense to the normal testis on the T2-weighted image and hyperintense on the T1-weighted image. **(c)** Axial fat-suppressed T1-weighted MR image shows a loss of high T1 signal intensity, a finding suggestive of internal fat content (arrow). **(d)** Coronal gadolinium-enhanced fat-suppressed T1-weighted MR image shows avid but heterogeneous enhancement of the lesion (arrow). Considering the internal fat content, an imaging diagnosis of intratesticular lipoma or teratoma was suggested. Postorchiectomy histologic analysis demonstrated a testicular adrenal rest tumor.

Testicular Adrenal Rest Tumor

Testicular adrenal rests are benign intratesticular lesions derived from displaced cells of the primordial adrenal gland. They occur in 29% of patients with congenital adrenal hyperplasia (CAH), an autosomal recessive disease characterized by a deficiency of adrenal cortical enzymes such as 21-hydroxylase (60). An increase in the adrenocorticotropic hormone (ACTH) level causes hyperplasia of the adrenal remnant in the testis with CAH and results in development of intratesticular masses (61), which are typically located in the region of the mediastinum testis and are usually bilateral. The MR imaging features are nonspecific; tumors can appear isointense to the normal testicular parenchyma on T1-weighted images and hyperintense on T2-weighted images, with diffuse contrast enhancement (Fig 18) (60,62). At US, adrenal rest tumors appear as hypoechoic intratesticular masses with or without a posterior acoustic shadow, depending on the degree of fibrosis. Recognizing an adrenal rest tumor as an intratesticular mass is important in patients with CAH because the appropriate treatment is glucocorticoid therapy rather than surgery, and the tumor may shrink after glucocorticoid therapy, which supports the diagnosis (60). At histologic analysis, it is difficult to diagnose adrenal rest tumors because they resemble Leydig cell tumors. Adrenal steroid metabolite measurement through testicular vein sampling provides the most conclusive information (60).

Testicular Malakoplakia

Testicular malakoplakia is a rare benign condition that occurs in immunocompromised patients with chronic infection, often *Escherichia coli* infection (63,64). Malakoplakia usually affects the urinary bladder, but the testes are affected in 12% of cases; the average age at occurrence is 50 years (64). Patients usually present with epididymo-orchitis or testicular enlargement with fibrous consistency and soft areas. The condition is characterized by von Hansemann cells and intracytoplasmic inclusion bodies called Michaelis-Gutmann (MG) bodies, which are

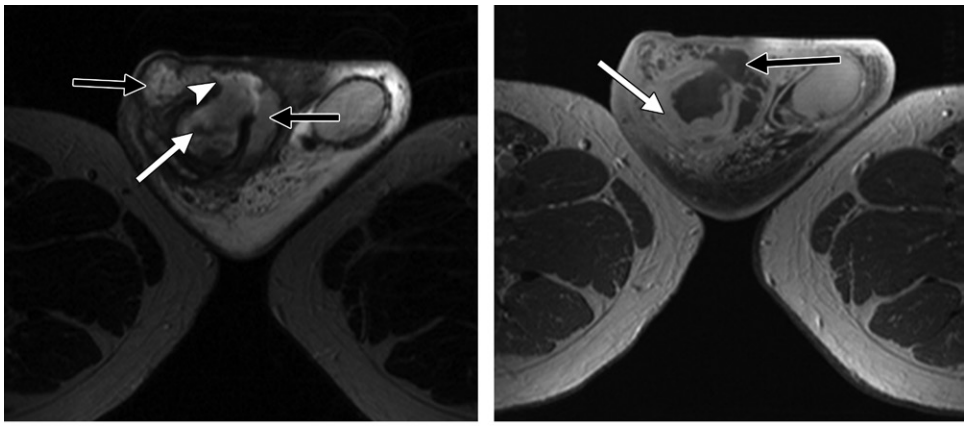

a. b.

Figure 19. Malakoplakia in a 44-year-old man with a clinical suspicion for epididymo-orchitis. **(a)** Axial T2-weighted MR image shows an enlarged right testis (white arrow) with heterogeneous signal intensity. An area of T2-hyperintense content (black arrows) is noted inferior and lateral to the right testis and demonstrates communication with the right testis (arrowhead). These features suggest an intratesticular abscess with paratesticular extension. **(b)** Axial contrast-enhanced fat-suppressed T1-weighted MR image shows thick irregular rim enhancement of the testis (white arrow) and the paratesticular abscess (black arrow). Postorchiectomy histologic analysis revealed malakoplakia.

the pathognomonic findings for malakoplakia (63,65). Surgery is the only way to differentiate malakoplakia from malignant or other infectious processes (63). At imaging, there is unilateral testicular enlargement with a focal intratesticular mass with cystic cavities (Fig 19). Epididymal involvement occurs in some cases. Intratesticular abscesses and vascular thrombosis can occur, although intratesticular abscesses are commonly encountered in the setting of acute bacterial epididymitis (64,65). Diagnosis of malakoplakia can be challenging because the condition often masquerades as a neoplastic process owing to the masslike manifestation. The differential diagnosis includes xanthogranulomatous inflammation and Rosai-Dorfman disease, both of which lack MG bodies. Xanthogranulomatous inflammation has a giant cell component, whereas Rosai-Dorfman disease is characterized by S-100 positive histiocytes containing phagocytized mononuclear cells (emperipolesis). Orchitis, torsion, and infarction are other conditions that should be included in the differential diagnosis (64).

Malignant Testicular Tumors

Testicular cancer is one of the few malignancies that can be cured even after metastases have occurred. MR imaging is usually recommended as a problem-solving modality to provide information regarding preoperative localization, characterization, and the histologic nature of various benign intratesticular mass lesions, including the presence of fat, fluid, hemorrhage, fibrous tissue, and solid contrast-enhancing tissue, findings that help narrow the differential diagnosis and determine patient care. The 5-year survival rate according to local, regional, or distant metastatic disease is 99.2%, 96.0%, or 73.1%, respectively. The overall 5-year survival rate for all stages of testicular cancer is 96.6% (66). Testicular carcinoma represents only 1%–1.5% of all malignancies in men but is the most common neoplasm in the 15–34-year age group (3). Ninety-five percent of testicular tumors are germ cell tumors arising from the germinal epithelium of seminiferous tubules, and these tumors are almost evenly split between seminomas and nonseminomatous germ cell tumors (1). Fewer than 50% of malignant germ cell tumors have a single cell type, of which 50% are seminoma. The remaining tumors have more than one cell type. Nonseminomatous germ cell tumors are histologically diverse neoplasms, including embryonal carcinoma, yolk sac tumor, teratoma, and choriocarcinoma; most are mixed germ cell tumors (MGCTs). Until 2016, the classification of testicular tumors was based on the morphology of the neoplasm. In 2016, the WHO published an updated classification of tumors of the urinary system and male genital organs according to whether the tumors are derived from germ cell neoplasia in situ (GCNIS) or are unrelated to GCNIS (Table 2) (67). Seminoma is considered a GCNIS-derived tumor. Before the 2016 WHO classification, spermatocytic seminoma was considered a subtype of seminoma; however, since it lacks association with GCNIS, it is now considered a separate entity unrelated to seminoma (67).

Seminoma

Seminoma is the most common subtype of testicular cancer, accounting for 30%–50% of all germ cell tumors. Seminoma is usually diagnosed in

patients a decade later than nonseminomatous germ cell tumors, with a median age of 35–39 years at diagnosis (68). Approximately 75% of patients present with disease limited to the testis, 20% have retroperitoneal adenopathy, and 5% have extragonadal metastasis. Seminomas range in size from small well-defined nodules to large masses replacing the entire testis, making it difficult to differentiate seminomas from other infiltrative masses of the testis, such as lymphoma and leukemia (47). Rarely they are multifocal. Bilateral tumors are rare, occurring in only 2% of cases, and are usually synchronous (3). Seminoma is extremely radiosensitive, resulting in a 5-year survival rate of 95%. Patients with advanced-stage disease may require chemotherapy followed by radiation. Histologically, tumor cells are uniform, with an abundant clear cytoplasm arranged in nests outlined by fibrous bands associated with lymphocytic infiltrate. At T2-weighted MR imaging, seminomas are often multinodular, with relatively homogeneous hypointense signal relative to the normal testis. At T1- or T2-weighted imaging, bandlike structures or fibrovascular septa may be seen as low-signal-intensity areas that enhance more than the remaining tumor after contrast agent administration. At diffusion-weighted imaging, seminomas are hyperintense with corresponding low values on the ADC map owing to high tumor cellularity, densely packed neoplastic cells, and enlargement of nuclei resulting in reduced water molecule motility (restricted diffusion) (Fig 20) (69).

Nonseminomatous Germ Cell Tumors

Embryonal Carcinoma.—Embryonal carcinoma is the second most common testicular tumor after seminoma. It is present in 87% of mixed germ cell tumors (MGCTs); the pure form of embryonal cell carcinoma accounts for only 2%–3% of testicular tumors (3,70). It occurs in younger men (median age, 25-35 years) than does seminoma (70). Embryonal carcinoma is derived from primitive anaplastic cells, reflecting early embryonic cells. It is mainly a solid tumor, is usually smaller than a seminoma, and may contain foci of necrosis and hemorrhage. Embryonal carcinoma tends to be aggressive in behavior (3,70,71) and usually produces α-fetoprotein (AFP). At MR imaging, embryonal carcinoma is heterogeneous, with areas of necrosis and hemorrhage, and is poorly marginated because of invasion of the tunica albuginea; the borders of the tumor are less distinct because of infiltration and blending with adjacent parenchyma, which give the testis a lobulated appearance (Fig 21) (3,52).

Table 2: Updated 2016 WHO Classification of Testicular Germ Cell Tumors

GCNIS-derived tumors:
Seminoma
Embryonal carcinoma
Yolk sac tumor
Choriocarcinoma
Teratoma (postpubertal)
Non–GCNIS-derived tumors:
Spermatocytic tumor
Prepubertal-type yolk sac tumor
Prepubertal-type teratoma

Source.—Reference 67.
Note.—GCNIS = germ cell neoplasia in situ.

Yolk Sac Tumor.—Yolk sac tumors, also known as endodermal sinus tumors, develop from totipotent germ cells. Yolk sac tumor is the most common childhood testicular tumor diagnosed before the age of 2 years (72). Yolk sac tumors in their pure form are rare in adults; 44% of cases of MGCTs in adults contain this cell type. Elevated AFP levels are present in 90% of patients with yolk sac tumors, as AFP is mainly produced by the embryonic yolk sac (73). The imaging findings are nonspecific, and treatment is similar to that of other nonseminomatous germ cell tumors.

Choriocarcinoma.—Choriocarcinoma is a highly malignant form of testicular carcinoma manifesting as tiny foci in 8% of MGCTs (3,52,70,74). The pure form occurs in less than 1% of patients, commonly in the 2nd or 3rd decade of life (3). Choriocarcinomas are composed of cytotrophoblastic and syncytiotrophoblastic cells that produce human chorionic gonadotropins (52,75). Because of microvascular invasion, there is early widespread metastasis to the lungs, liver, gastrointestinal tract, and brain. Patients may present with symptoms referable to the metastases earlier than symptoms related to the testicular mass. The primary lesion and metastases are often heterogeneous and particularly necrotic and appear so on imaging studies.

Teratoma.—Teratomas contain elements of all three germ cell layers: endoderm, mesoderm, and ectoderm (75). Teratomas can occur in any age group; after yolk sac tumor, pure teratoma is the second most common testicular tumor in children. Because prepubertal-type teratomas are benign, testicular-sparing enucleation is recommended instead of orchiectomy in prepubertal boys (76,77). In its pure form, teratoma is rare in adults and represents only 2%–3% of testicular

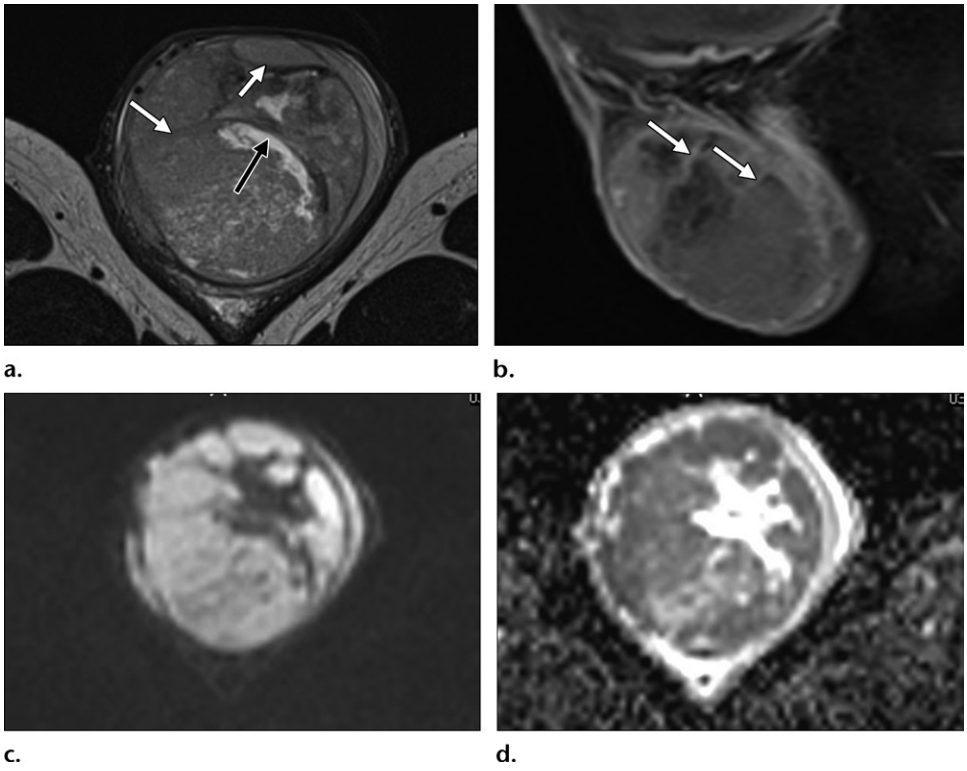

Figure 20. Seminoma in a 34-year-old man who presented with a hard scrotal mass. **(a)** Axial T2-weighted MR image shows a hypointense, lobulated, multinodular well-defined lesion in the right testis with bandlike low-signal-intensity fibrovascular septa (white arrows) and central T2 hyperintensity due to necrosis (black arrow). **(b)** Sagittal contrast-enhanced T1-weighted MR image shows greater enhancement of the septa (arrows) in comparison with the mass. **(c)** Axial diffusion-weighted MR image (b = 800 sec/mm^2) shows the mass with high signal intensity. **(d)** ADC map shows low signal intensity from restricted diffusion in the mass. Postorchiectomy histologic analysis revealed pure seminoma.

neoplasms; however, teratomatous components occur in approximately half of adult cases of mixed tumors (52). Teratomas in adults, regardless of age, should be considered malignant (52). These tumors are subdivided into mature, immature, and those with malignant transformation (3,74). Although dermoids represent the most common teratomatous lesions in the ovary, they constitute a small minority of testicular teratomas. Irrespective of the histopathologic characteristics, every element in an adult teratoma, whether mature or immature, can metastasize; therefore, nonteratomatous elements can be present in metastases (3). Teratomas are generally well-circumscribed complex cystic masses with variable signal intensity characteristics depending on the contents (serous, mucous, and keratinous fluids). The cystic portion can be complex at imaging. Cartilage, calcifications, fibrosis, and scar formation result in a heterogeneous appearance. The imaging features of mature and immature teratomas usually overlap, making them difficult to differentiate (2). Mature teratomas are predominantly cystic and are lined with epithelium with resulting dermal appendages; 93% contain sebaceous fat (Fig 22) (2). Immature teratomas are largely encapsulated, with rich solid areas composed of immature neuroectodermal components (2,75). Fifty percent of cases have increased levels of AFP. At MR imaging, malignant teratomas demonstrate heterogeneous contrast enhancement (Fig 23).

Mixed Germ Cell Tumors

MGCTs are malignant tumors that contain more than one germ cell component or histologic subtypes of all germ cell tumors; the most malignant governs the prognosis (3,70,75,78). The average patient age at presentation is 30 years, and although any cell type combination is possible, embryonal carcinoma is the most common component and is often combined with one or more components (teratoma, seminoma, yolk sac tumor, and choriocarcinoma). MGCTs constitute 69% of all nonseminomatous germ cell tumors, even if the seminomatous component predominates, and 32% of all testicular germ cell tumors (18). These tumors rarely occur in prepubertal patients. Tumor marker elevation is a reflection of the individual tumor components; AFP elevations occur in 60% of cases, and β–human chorionic gonadotropin

a.

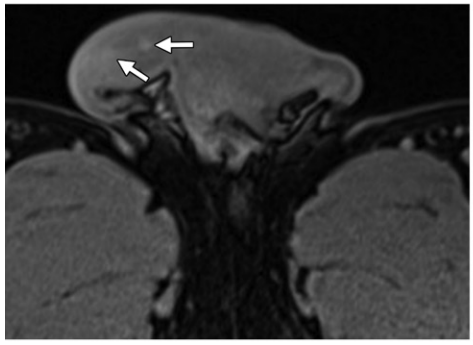

b.

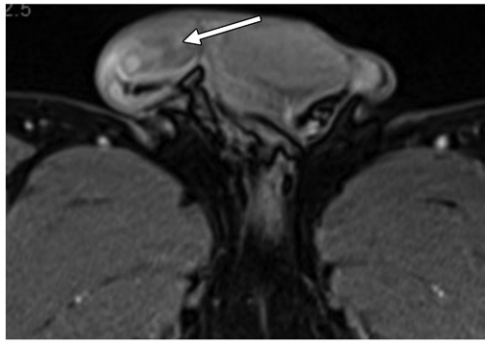

c.

Figure 21. Embryonal carcinoma in a 30-year-old man who presented with a painless right scrotal mass. **(a)** Coronal T2-weighted MR image shows a lobulated heterogeneous mass (arrows) with areas of low signal intensity that invades the tunica albuginea. **(b)** Corresponding axial nonenhanced T1-weighted MR image shows areas of high signal intensity due to hemorrhage (arrows). **(c)** Axial contrast-enhanced T1-weighted MR image shows heterogeneous enhancement of the mass (arrow).

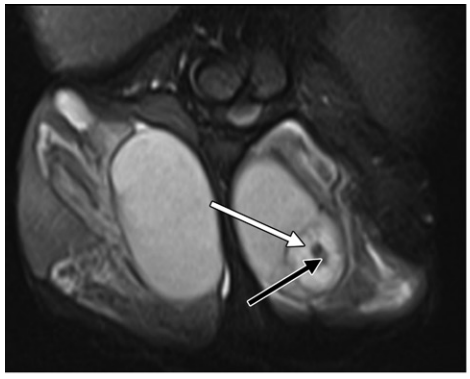

a.

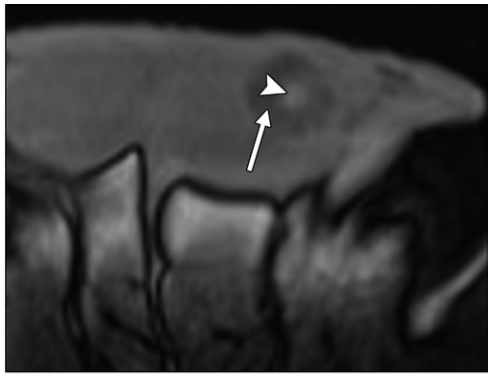

b.

Figure 22. Mature teratoma in a 40-year-old man with a left testicular mass. **(a)** Coronal T2-weighted MR image through the scrotum shows a well-defined lesion in the left testis with a hyperintense outer rim (white arrow) and central hypointensity (black arrow). **(b)** Corresponding axial fat-suppressed T1-weighted MR image reveals hypointensity of the outer rim (arrow) due to fat and internal hyperintensity (arrowhead) due to blood products, findings consistent with a fat-containing mature teratoma.

(β-HCG) levels are elevated in 55% of patients (79). Radiologic findings are variable depending on the proportions of each tumor type. The heterogeneous tumor appearance is caused by hemorrhage, necrosis, or a combination of the two. Calcifications are present in over 40% of cases (79). At MR imaging, MGCTs are heterogeneous in signal intensity, depending on the histologic component and the presence of hemorrhage (Fig 24).

Spermatocytic Tumor

According to the new WHO classification, spermatocytic tumor is considered unrelated

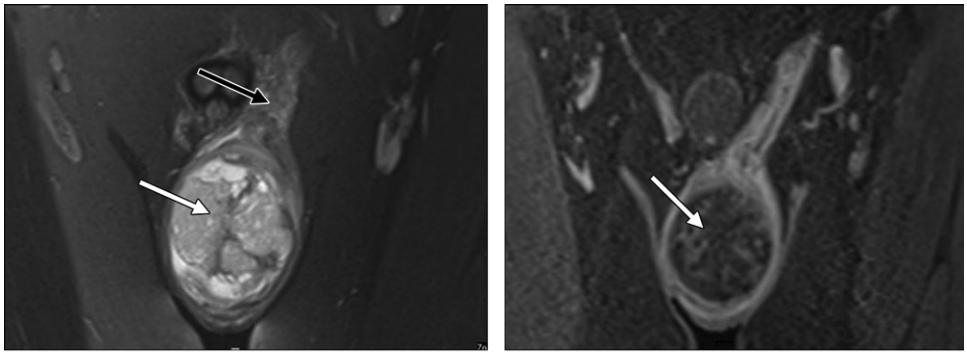

a. b.

Figure 23. Malignant teratoma in a 35-year-old man with a painless left testicular mass. **(a)** Coronal fat-suppressed T2–weighted MR image through the scrotum shows a heterogeneous cystic and solid lesion (white arrow) involving the left testis, with thickening of the spermatic cord (black arrow). **(b)** Coronal contrast-enhanced T1-weighted MR image shows heterogeneous enhancement of the lesion (arrow). Postorchiectomy histologic analysis revealed malignant teratoma.

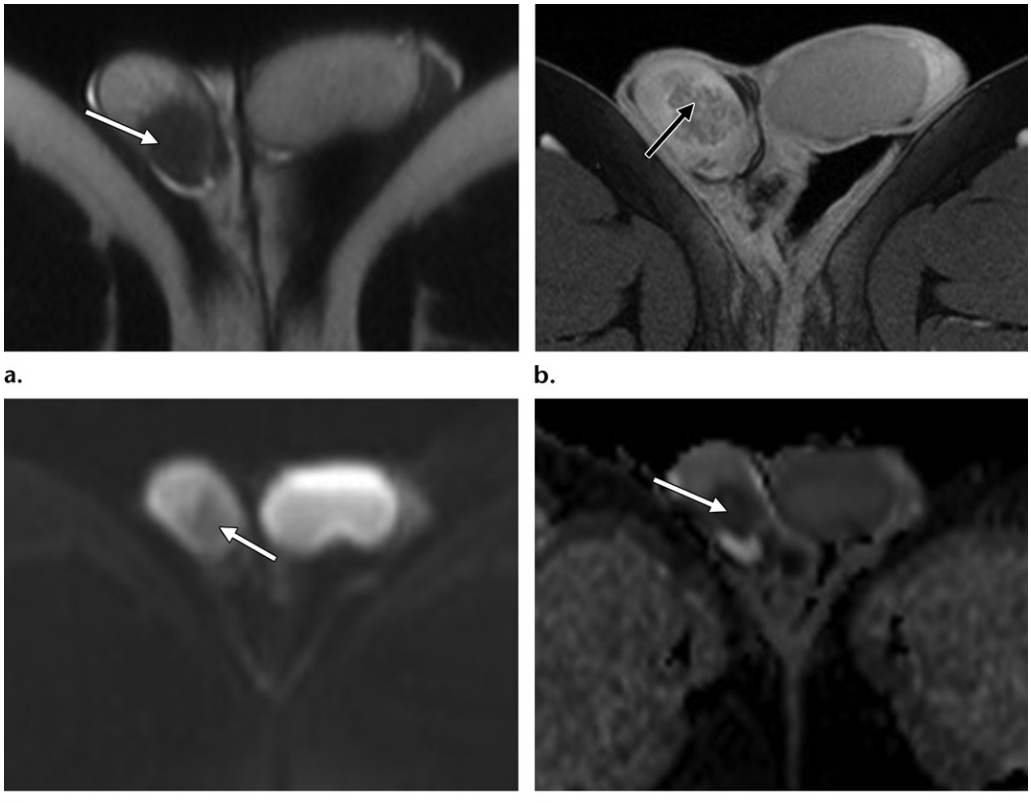

a. b. c. d.

Figure 24. Malignant MGCT in a 32-year-old man with a right testicular mass. **(a)** Axial T2-weighted MR image shows an ill-defined hypointense mass (arrow) in the right testis. **(b)** Axial contrast-enhanced T1-weighted MR image shows heterogeneous enhancement of the lesion (arrow). **(c, d)** Axial diffusion-weighted MR image (b = 800 sec/mm^2) **(c)** and ADC map **(d)** show restricted diffusion in the mass (arrow). Postorchiectomy histologic analysis revealed malignant MGCT.

to classic seminoma and is not associated with cryptorchidism (67,80). It more often occurs in older men than does classic seminoma, with a median age at diagnosis of 54 years (67). The tumor is usually larger than 5 cm at diagnosis and is unilateral in 90% of cases (81). At histologic analysis, spermatocytic tumors are composed of a mixture of small to large giant cells, which may be multinucleated. The tumor cells lack glycogenation, which is a feature of seminoma. The tumor shows positivity to SALL4, but C-Kit is positive in only 50% of cases; there is no reaction to OCT3/4 (67,82). At imaging, a spermatocytic tumor is well defined but heterogeneous and may contain cystic spaces with a gelatinous appearance (81).

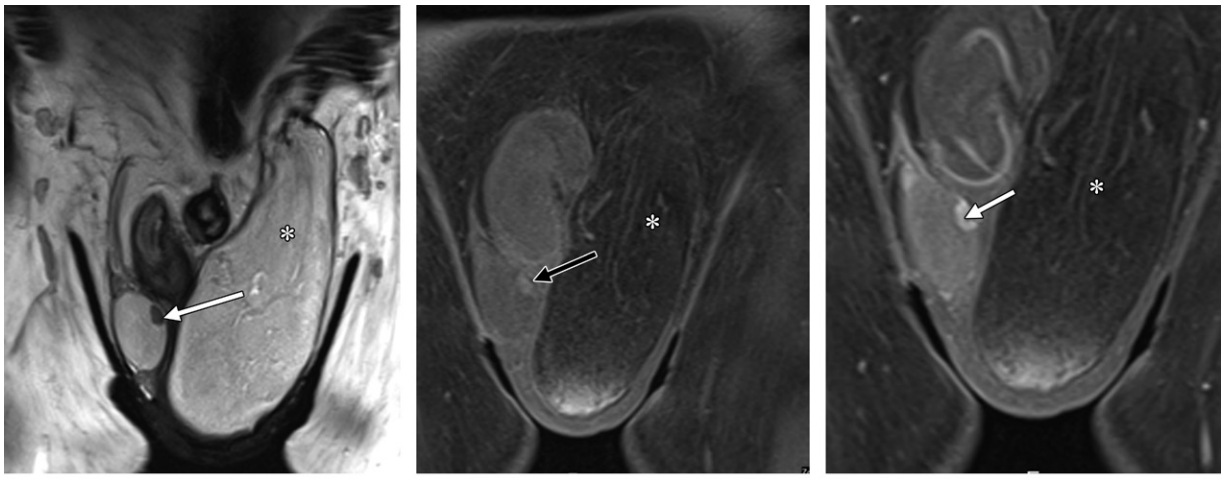

a. b. c.

Figure 25. Leydig cell tumor in a 35-year-old man who presented with gynecomastia and decreased libido. ∗ = incidental fat-containing left inguinal hernia. **(a)** Coronal T2-weighted MR image shows a hypointense nodule (arrow) in the right testis. **(b)** Corresponding nonenhanced T1-weighted MR image shows the mass (arrow) as nearly isointense to the testicular parenchyma. **(c)** Coronal contrast-enhanced T1-weighted MR image shows marked enhancement of the mass (arrow).

Non–Germ Cell Tumors

Sex Cord–Stromal Tumors

Sex cord–stromal tumors comprise about 5% of testicular tumors in adults but up to 30% of all testicular tumors in children. They arise from the cells forming sex cord and interstitial stroma. In a patient who presents with a testicular mass and findings of endocrinopathy, a sex cord–stromal tumor should be considered. These tumors include Leydig cell, Sertoli cell, and granulosa cell tumors (83,84).

Leydig Cell Tumor.—Leydig cell tumors are the most common sex cord–stromal tumors, comprising 1%–3% of all testicular tumors (84). These tumors arise from the sex cord interstitium. Leydig cell tumors occur in all age groups, but the peak incidences are at ages 5–10 years and 30–35 years (3,84). Leydig cells are the principal source of testosterone and are under the stimulating influence of luteinizing hormone. They are also capable of estrogen production by way of the aromatase enzyme complex (84). Therefore, because of androgen and estrogen secretion by the tumor, approximately 30% of patients present with signs of feminizing or virilizing syndrome, such as precocious puberty, gynecomastia, and decreased libido.

At US, Leydig cell tumors are typically small hyperechoic or hypoechoic nodules. At MR imaging, these tumors are isointense relative to the normal testis on T1-weighted images, are hypointense on T2-weighted images, and show marked contrast enhancement (Fig 25). These tumors can also demonstrate a T2-hyperintense capsule or high signal intensity in the center because of cystic change (73). Therefore, these tumors can be indistinguishable from germ cell tumors (85). Leydig cell tumors can be pure or can be mixed with other stromal cell tumors or germ cell tumors. They primarily are benign, but malignant varieties can occur. Recently, an association with Klinefelter syndrome has been demonstrated (86). Although they once were treated with radical orchiectomy, Leydig cell tumors have been treated more recently with enucleation (87).

Sertoli Cell Tumor.—Sertoli cell tumors are sex cord–stromal neoplasms and constitute less than 1% of testicular tumors (2). Sertoli cell tumors typically occur in the first 4 decades of life. Most Sertoli cell tumors are benign, although in 10%–15% of cases they are malignant and metastasize. Pathologically, it is difficult to distinguish benign from malignant types. There are four histologic types: large cell calcifying, sclerosing, sex cord with annular tubules, and not otherwise specified (52,88). Gynecomastia in association with a testicular tumor in the pediatric population is an important finding that develops owing to stimulation of breast tissue from estrogen (distinct from lipomastia seen in overweight boys). Virilization is rarely associated with Sertoli cell tumor (84). Other signs of feminization or hyperestrogenism may be present. Large cell calcifying Sertoli cell tumors are mostly seen in prepubertal boys and have been associated with Peutz-Jeghers syndrome and Carney complex (3,84). Compared to other testicular tumors, which are usually single and unilateral, large cell calcified Sertoli cell tumors are multifocal and bilateral in 20% of cases (89). At US, the tumor appearance is variable and can include a multicystic spoke-wheel appearance or increased echogenicity caused by

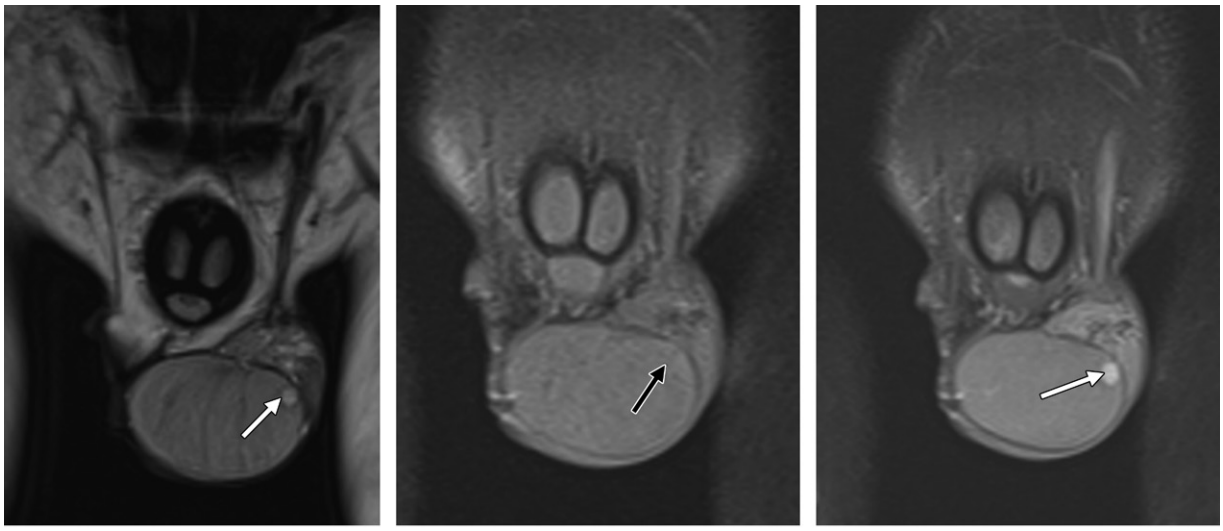

a. b. c.

Figure 26. Sertoli cell tumor in a 19-year-old man with prior right orchiectomy for Sertoli cell tumor who presented with gynecomastia and testicular pain. **(a)** Coronal T2-weighted MR image shows a hyperintense nodule (arrow) in the left testis. **(b)** Coronal nonenhanced T1-weighted MR image shows the nodule (arrow) as nearly isointense to the testicular parenchyma. **(c)** Coronal contrast-enhanced T1-weighted MR image shows marked contrast enhancement of the nodule (arrow).

the dense collagenous matrix (90). MR imaging of Sertoli cell tumor demonstrates homogeneous intermediate T1 signal intensity, high T2 signal intensity, and homogeneous enhancement (Fig 26).

Granulosa Cell Tumor.—Granulosa cell tumors of the testes are rare sex cord–stromal tumors, comparable to granulosa cell tumors of the ovary but far less common (84). These tumors are divided into adult and juvenile types.

Juvenile granulosa cell tumors are benign and rare but are the most frequent congenital testicular neoplasms occurring in infants younger than 6 months. The adult type is the least common type of sex cord–stromal tumors, with a median patient age of 44 years. These tumors are considered benign tumors, but metastases have been reported. They are slow-growing tumors, but distant metastasis can be seen years after the initial diagnosis (91). These tumors usually occur in white males and present as a painless testicular mass. Gynecomastia is present in 25% of cases and is due to estrogen hypersecretion or chromosomal abnormalities (92). At US, the mass is well defined and hypoechoic, with few internal echoes and increased peripheral and low central vascularity. At MR imaging, the mass demonstrates hypointense signal on T2-weighted images, hypo- to isointense signal on T1-weighted images, and intense contrast enhancement (Fig 27).

Testicular Lymphoma

Testicular lymphoma is the most common testicular malignancy in men older than 60 years, accounting for 50% of cases in this age group (47,52). Testicular lymphoma constitutes 1%–9% of all testicular tumors, with most being diffuse large B-cell non-Hodgkin lymphomas (1,2). Secondary involvement of the testis in patients with established lymphoma is much more common than is primary testicular lymphoma (1,3). Testicular lymphoma is the most common bilateral neoplasm, with a 20% prevalence of the synchronous type; however, the metachronous type is much more common, involving the contralateral testis months to years after orchiectomy (93). Although the predisposing factors for development of lymphoma are unclear, immunocompromised patients are at risk for development of extranodal lymphoma, including in the testis, at a younger age (94). Lymphoma is often locally invasive, infiltrating the epididymis, spermatic cord, and scrotal skin (93,95). Although the infiltrative pattern is the most common, testicular lymphoma can manifest as focal masses (2). The differential diagnosis includes epididymitis, sarcoidosis, and leukemia. Inflammatory processes such as epididymo-orchitis are tender at physical examination but improve after treatment with antibiotics, whereas lymphoma or other testicular tumors are painless and do not resolve after treatment but can demonstrate interval growth (94). Testicular sarcoid is more common in African-American males and does not respond to antibiotics. Testicular lymphoma can be an infiltrative process and can affect patients with a previous history of leukemia (93). At T1- and T2-weighted MR imaging, testicular lymphoma demonstrates low signal intensity

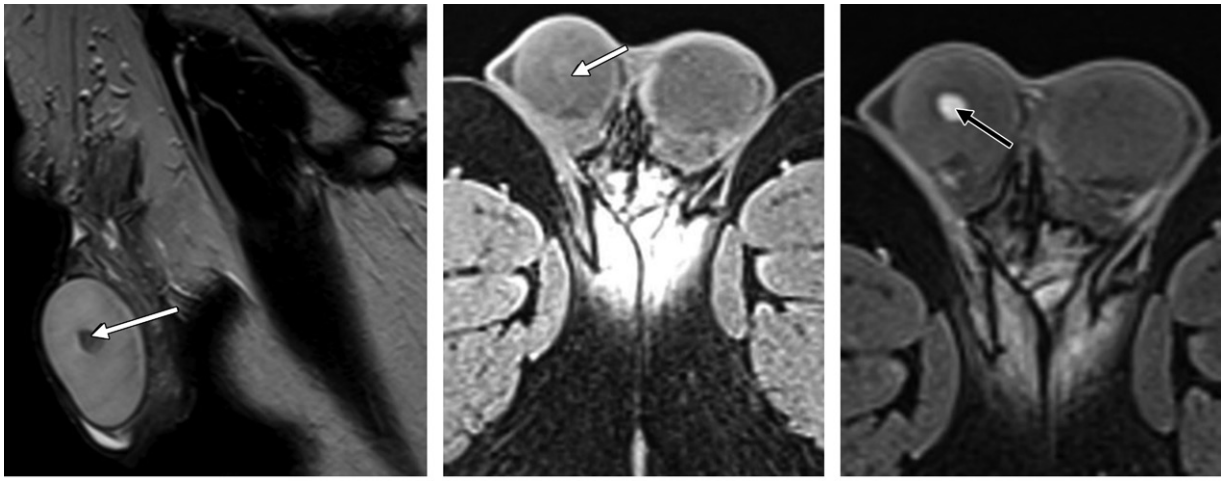

a. b. c.

Figure 27. Granulosa cell tumor in a 40-year-old man who presented with gynecomastia and a painless mass in the right testis. **(a)** Sagittal T2-weighted MR image shows a hypointense nodule (arrow) in the right testis. **(b)** Axial nonenhanced T2-weighted MR image shows the nodule (arrow) as isointense relative to the testicular parenchyma. **(c)** Axial contrast-enhanced T1-weighted MR image shows marked enhancement of the nodule (arrow).

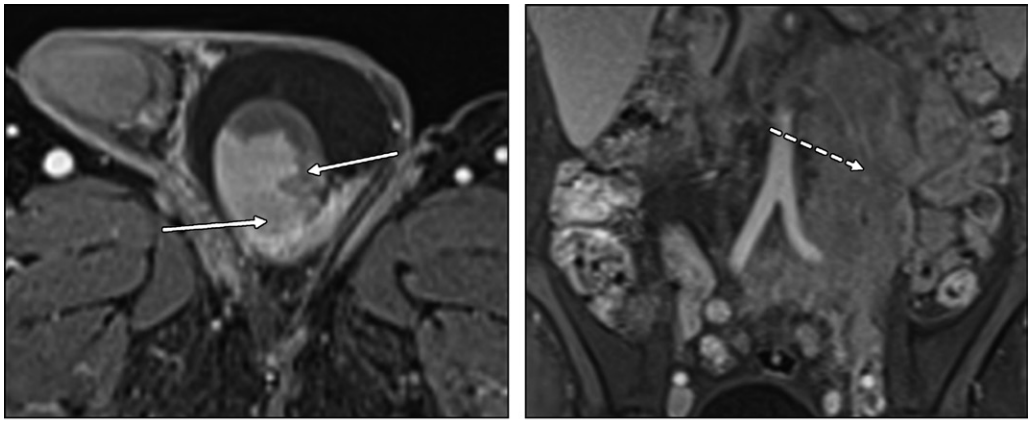

a. b.

Figure 28. Lymphoma in a 68-year-old man with left-sided scrotal swelling. **(a)** Axial contrast-enhanced fat-suppressed T1-weighted MR image shows a hypointense infiltrative lesion (arrows) in the left testis that enhances less than the normal testis. **(b)** Coronal contrast-enhanced fat-suppressed T1-weighted MR image of the abdomen shows an enlarged conglomerate of lymph nodes in the left retroperitoneum (arrow).

with less contrast enhancement than the normal testis and also shows restricted diffusion (Fig 28).

Conclusion

Although US is the first-line imaging modality for investigation of scrotal lesions, MR imaging of the scrotum has proven to be an effective adjunct diagnostic tool in the characterization and localization of masses, especially when the US findings are inconclusive. The superior soft-tissue contrast and multiplanar capabilities of MR imaging help in the depiction of intralesional architecture, such as cystic or solid areas, fat, blood, and fibrosis. It is important for radiologists and urologists to understand the features of benign and malignant conditions of the scrotum and the role of MR imaging in the presurgical workup of scrotal masses, which affects patient care and management.

References

1. Tsili AC, Giannakis D, Sylakos A, Ntorkou A, Sofikitis N, Argyropoulou MI. MR imaging of scrotum. Magn Reson Imaging Clin N Am 2014;22(2):217–238, vi.
2. Cassidy FH, Ishioka KM, McMahon CJ, et al. MR imaging of scrotal tumors and pseudotumors. RadioGraphics 2010;30(3):665–683.
3. Woodward PJ, Sohaey R, O'Donoghue MJ, Green DE. Tumors and tumorlike lesions of the testis: radiologic-pathologic correlation. RadioGraphics 2002;22(1):189–216.
4. Tsili AC, Bertolotto M, Turgut AT, et al. MRI of the scrotum: recommendations of the ESUR Scrotal and Penile Imaging Working Group. Eur Radiol 2018;28(1):31–43.
5. Parker RA 3rd, Menias CO, Quazi R, et al. MR imaging of the penis and scrotum. RadioGraphics 2015;35(4):1033–1050.
6. Woodward PJ, Schwab CM, Sesterhenn IA. Extratesticular scrotal masses: radiologic-pathologic correlation. RadioGraphics 2003;23(1):215–240.

7. Müller-Leisse C, Bohndorf K, Stargardt A, et al. Gadolinium-enhanced T1-weighted versus T2-weighted imaging of scrotal disorders: is there an indication for MR imaging? J Magn Reson Imaging 1994;4(3):389–395.
8. Algebally AM, Tantawy HI, Yousef RR, Szmigielski W, Darweesh A. Advantage of adding diffusion weighted imaging to routine MRI examinations in the diagnostics of scrotal lesions. Pol J Radiol 2015;80:442–449.
9. Tsili AC, Giannakis D, Sylakos A, et al. Apparent diffusion coefficient values of normal testis and variations with age. Asian J Androl 2014;16(3):493–497.
10. Akbar SA, Sayyed TA, Jafri SZ, Hasteh F, Neill JS. Multimodality imaging of paratesticular neoplasms and their rare mimics. RadioGraphics 2003;23(6):1461–1476.
11. Park SB, Lee WC, Kim JK, et al. Imaging features of benign solid testicular and paratesticular lesions. Eur Radiol 2011;21(10):2226–2234.
12. Gooding GA. Sonography of the spermatic cord. AJR Am J Roentgenol 1988;151(4):721–724.
13. Cramer BM, Schlegel EA, Thueroff JW. MR imaging in the differential diagnosis of scrotal and testicular disease. RadioGraphics 1991;11(1):9–21.
14. Leonhardt WC, Gooding GA. Sonography of intrascrotal adenomatoid tumor. Urology 1992;39(1):90–92.
15. Garriga V, Serrano A, Marin A, Medrano S, Roson N, Pruna X. US of the tunica vaginalis testis: anatomic relationships and pathologic conditions. RadioGraphics 2009;29(7):2017–2032.
16. Patel MD, Silva AC. MRI of an adenomatoid tumor of the tunica albuginea. AJR Am J Roentgenol 2004;182(2):415–417.
17. de Klerk DP, Nime F. Adenomatoid tumors (mesothelioma) of testicular and paratesticular tissue. Urology 1975;6(5):635–641.
18. Kim W, Rosen MA, Langer JE, Banner MP, Siegelman ES, Ramchandani P. US MR imaging correlation in pathologic conditions of the scrotum. RadioGraphics 2007;27(5):1239–1253.
19. Germaine P, Simerman LP. Fibrous pseudotumor of the scrotum. J Ultrasound Med 2007;26(1):133–138.
20. Sajjad SM, Azizi MR, Llamas L. Fibrous pseudotumor of testicular tunic. Urology 1982;19(1):86–88.
21. Bhatt S, Rubens DJ, Dogra VS. Sonography of benign intrascrotal lesions. Ultrasound Q 2006;22(2):121–136.
22. Wolfman DJ, Marko J, Gould CF, Sesterhenn IA, Lattin GE Jr. Mesenchymal extratesticular tumors and tumorlike conditions. RadioGraphics 2015;35(7):1943–1954.
23. Bhatt S, Dogra VS. Role of US in testicular and scrotal trauma. RadioGraphics 2008;28(6):1617–1629.
24. Pepe P, Panella P, Pennisi M, Aragona F. Does color Doppler sonography improve the clinical assessment of patients with acute scrotum? Eur J Radiol 2006;60(1):120–124.
25. Michaelides M, Sotiriadis C, Konstantinou D, Pervana S, Tsitouridis I. Tuberculous orchitis US and MRI findings: correlation with histopathological findings. Hippokratia 2010;14(4):297–299.
26. Muttarak M, Peh WC. Case 91: tuberculous epididymo-orchitis. Radiology 2006;238(2):748–751.
27. Chung JJ, Kim MJ, Lee T, Yoo HS, Lee JT. Sonographic findings in tuberculous epididymitis and epididymo-orchitis. J Clin Ultrasound 1997;25(7):390–394.
28. Amodio JB, Maybody M, Slowotsky C, Fried K, Foresto C. Polyorchidism: report of 3 cases and review of the literature. J Ultrasound Med 2004;23(7):951–957.
29. Bergholz R, Wenke K. Polyorchidism: a meta-analysis. J Urol 2009;182(5):2422–2427.
30. Sağlam HS, Önol FF, Avcı E, Ergüven A. Report of a boy with polyorchidism and a review of current knowledge regarding this unusual anomaly. Turk J Urol 2013;39(2):119–121.
31. Hirokawa M, Monobe Y, Shimizu M, Terayama K, Kanahara T, Manabe T. Sclerosing lipogranuloma of the scrotum: report of a case with fine needle aspiration biopsy findings. Acta Cytol 1998;42(5):1181–1183.
32. Tsili AC, Xiropotamou ON, Nomikos M, Argyropoulou MI. Silicone-induced penile sclerosing lipogranuloma: magnetic resonance imaging findings. J Clin Imaging Sci 2016;6(1):3.
33. Ricchiuti VS, Richman MB, Haas CA, Desai D, Cai DX. Sclerosing lipogranuloma of the testis. Urology 2002;60(3):515.
34. Mungan S, Karagüzel E, Turan C, Reıs A. A giant primary sclerosing lipogranuloma of the scrotum. Turk Patoloji Derg 2014;30(1):78–80.
35. Nishizawa K, Kobayashi T, Ogura K, Ide Y, Togashi K. Magnetic resonance imaging of sclerosing lipogranuloma of male genitalia. J Urol 2002;168(4 pt 1):1500–1501.
36. Rodríguez D, Olumi AF. Management of spermatic cord tumors: a rare urologic malignancy. Ther Adv Urol 2012;4(6):325–334.
37. Sogani PC, Grabstald H, Whitmore WF Jr. Spermatic cord sarcoma in adults. J Urol 1978;120(3):301–305.
38. Gregorio MD, D'Hondt L, Lorge F, Nollevaux MC. Liposarcoma of the spermatic cord: an infrequent pathology. Case Rep Oncol 2017;10(1):136–142.
39. Montgomery E, Fisher C. Paratesticular liposarcoma: a clinicopathologic study. Am J Surg Pathol 2003;27(1):40–47.
40. Schwartz SL, Swierzewski SJ 3rd, Sondak VK, Grossman HB. Liposarcoma of the spermatic cord: report of 6 cases and review of the literature. J Urol 1995;153(1):154–157.
41. Mason BJ, Kier R. Sonographic and MR imaging appearances of paratesticular rhabdomyosarcoma. AJR Am J Roentgenol 1998;171(2):523–524.
42. Hermans BP, Foster RS, Bihrle R, et al. Is retroperitoneal lymph node dissection necessary for adult paratesticular rhabdomyosarcoma? J Urol 1998;160(6 pt 1):2074–2077.
43. Tannous WN, Azouz EM, Homsy YL, Kiruluta HG, Grattan-Smith D. CT and ultrasound imaging of pelvic rhabdomyosarcoma in children: a review of 56 patients. Pediatr Radiol 1989;19(8):530–534.
44. Bhatt S, Jafri SZ, Wasserman N, Dogra VS. Imaging of non-neoplastic intratesticular masses. Diagn Interv Radiol 2011;17(1):52–63.
45. Bree RL, Hoang DT. Scrotal ultrasound. Radiol Clin North Am 1996;34(6):1183–1205.
46. Gupta R, Alobaidi M, Jafri SZ, Bis K, Amendola M. Correlation of US and MRI findings of intratesticular and paratesticular lesions: from infants to adults. Curr Probl Diagn Radiol 2005;34(1):35–45.
47. Aganovic L, Cassidy F. Imaging of the scrotum. Radiol Clin North Am 2012;50(6):1145–1165.
48. Avery LL, Scheinfeld MH. Imaging of penile and scrotal emergencies. RadioGraphics 2013;33(3):721–740.
49. Deurdulian C, Mittelstaedt CA, Chong WK, Fielding JR. US of acute scrotal trauma: optimal technique, imaging findings, and management. RadioGraphics 2007;27(2):357–369.
50. Bilagi P, Sriprasad S, Clarke JL, Sellars ME, Muir GH, Sidhu PS. Clinical and ultrasound features of segmental testicular infarction: six-year experience from a single centre. Eur Radiol 2007;17(11):2810–2818.
51. Fernández-Pérez GC, Tardáguila FM, Velasco M, et al. Radiologic findings of segmental testicular infarction. AJR Am J Roentgenol 2005;184(5):1587–1593.
52. Dogra VS, Gottlieb RH, Oka M, Rubens DJ. Sonography of the scrotum. Radiology 2003;227(1):18–36.
53. Lerner RM, Mevorach RA, Hulbert WC, Rabinowitz R. Color Doppler US in the evaluation of acute scrotal disease. Radiology 1990;176(2):355–358.
54. Prando D. Torsion of the spermatic cord: the main gray-scale and Doppler sonographic signs. Abdom Imaging 2009;34(5):648–661.
55. Watanabe Y, Nagayama M, Okumura A, et al. MR imaging of testicular torsion: features of testicular hemorrhagic necrosis and clinical outcomes. J Magn Reson Imaging 2007;26(1):100–108.
56. Fehily SR, Trubiano JA, McLean C, et al. Testicular loss following bacterial epididymo-orchitis: case report and literature review. Can Urol Assoc J 2015;9(3-4):E148–E151.
57. Saxon P, Badler RL, Desser TS, Tublin ME, Katz DS. Segmental testicular infarction: report of seven new cases and literature review. Emerg Radiol 2012;19(3):217–223.
58. Madaan S, Joniau S, Klockaerts K, et al. Segmental testicular infarction: conservative management is feasible and safe. Eur Urol 2008;53(2):441–445.
59. Shiraj S, Ramani N, Wojtowycz AR. Segmental testicular infarction, an underdiagnosed entity: case report with histopathologic correlation and review of the diagnostic features. Case Rep Radiol 2016;2016:8741632.

60. Avila NA, Premkumar A, Merke DP. Testicular adrenal rest tissue in congenital adrenal hyperplasia: comparison of MR imaging and sonographic findings. AJR Am J Roentgenol 1999;172(4):1003–1006.
61. Proto G, Di Donna A, Grimaldi F, Mazzolini A, Purinan A, Bertolissi F. Bilateral testicular adrenal rest tissue in congenital adrenal hyperplasia: US and MR features. J Endocrinol Invest 2001;24(7):529–531.
62. Stikkelbroeck NM, Suliman HM, Otten BJ, Hermus AR, Blickman JG, Jager GJ. Testicular adrenal rest tumours in postpubertal males with congenital adrenal hyperplasia: sonographic and MR features. Eur Radiol 2003;13(7):1597–1603.
63. Mannan AA, Kahvic M, Singh NG, Abu Sara Y, Bharati C. An unusual case of extensive epididymotesticular malakoplakia in a diabetic patient. Int Urol Nephrol 2010;42(3):569–573.
64. Morgan TA, Rabban JT, Filly RA. Testicular malakoplakia: a rare sonographic mimic of malignancy. J Clin Ultrasound 2015;43(3):199–202.
65. Dieckmann KP, Henke RP, Zimmer-Krolzig G. Malacoplakia of the epididymis: report of a case and review of the literature. Urol Int 1995;55(4):222–225.
66. Stevenson SM, Lowrance WT. Epidemiology and diagnosis of testis cancer. Urol Clin North Am 2015;42(3):269–275.
67. Williamson SR, Delahunt B, Magi-Galluzzi C, et al. The World Health Organization 2016 classification of testicular germ cell tumours: a review and update from the International Society of Urological Pathology Testis Consultation Panel. Histopathology 2017;70(3):335–346.
68. Trabert B, Chen J, Devesa SS, Bray F, McGlynn KA. International patterns and trends in testicular cancer incidence, overall and by histologic subtype, 1973-2007. Andrology 2015;3(1):4–12.
69. Tsili AC, Argyropoulou MI, Giannakis D, Tsampalas S, Sofikitis N, Tsampoulas K. Diffusion-weighted MR imaging of normal and abnormal scrotum: preliminary results. Asian J Androl 2012;14(4):649–654.
70. Secil M, Altay C, Basara I. State of the art in germ cell tumor imaging. Urol Oncol 2016;34(3):156–164.
71. Tsili AC, Tsampoulas C, Giannakopoulos X, et al. MRI in the histologic characterization of testicular neoplasms. AJR Am J Roentgenol 2007;189(6):W331–W337.
72. Frush DP, Sheldon CA. Diagnostic imaging for pediatric scrotal disorders. RadioGraphics 1998;18(4):969–985.
73. Ulbright TM, Young RH. Testicular and paratesticular tumors and tumor-like lesions in the first 2 decades. Semin Diagn Pathol 2014;31(5):323–381.
74. Akin EA, Khati NJ, Hill MC. Ultrasound of the scrotum. Ultrasound Q 2004;20(4):181–200.
75. Ueno T, Tanaka YO, Nagata M, et al. Spectrum of germ cell tumors: from head to toe. RadioGraphics 2004;24(2):387–404.
76. Rushton HG, Belman AB, Sesterhenn I, Patterson K, Mostofi FK. Testicular sparing surgery for prepubertal teratoma of the testis: a clinical and pathological study. J Urol 1990;144(3):726–730.
77. Shukla AR, Woodard C, Carr MC, et al. Experience with testis sparing surgery for testicular teratoma. J Urol 2004;171(1):161–163.
78. Cheng L, Lyu B, Roth LM. Perspectives on testicular germ cell neoplasms. Hum Pathol 2017;59:10–25.
79. Adham WK, Raval BK, Uzquiano MC, Lemos LB. Bilateral testicular tumors: seminoma and mixed germ cell tumor. RadioGraphics 2005;25(3):835–839.
80. Sharmeen F, Rosenthal MH, Howard SA. The management of retroperitoneal lymphadenopathy in spermatocytic seminoma of the testicle. Clin Imaging 2014;38(2):202–204.
81. Varela JR, Pombo F, Requejo I, Aguilera C, Bargiela A, Alvarez A. Spermatocytic seminoma: sonographic appearance. J Ultrasound Med 1996;15(8):607–609.
82. Howitt BE, Berney DM. Tumors of the testis: morphologic features and molecular alterations. Surg Pathol Clin 2015;8(4):687–716.
83. Conkey DS, Howard GC, Grigor KM, McLaren DB, Kerr GR. Testicular sex cord-stromal tumours: the Edinburgh experience 1988-2002, and a review of the literature. Clin Oncol (R Coll Radiol) 2005;17(5):322–327.
84. Dilworth JP, Farrow GM, Oesterling JE. Non-germ cell tumors of testis. Urology 1991;37(5):399–417.
85. Avery GR, Peakman DJ, Young JR. Unusual hyperechoic ultrasound appearance of testicular Leydig cell tumour. Clin Radiol 1991;43(4):260–261.
86. Soria JC, Durdux C, Chrétien Y, Sibony M, Damotte D, Housset M. Malignant Leydig cell tumor of the testis associated with Klinefelter's syndrome. Anticancer Res 1999;19(5C):4491–4494.
87. Henderson CG, Ahmed AA, Sesterhenn I, Belman AB, Rushton HG. Enucleation for prepubertal Leydig cell tumor. J Urol 2006;176(2):703–705.
88. Gourgari E, Saloustros E, Stratakis CA. Large-cell calcifying Sertoli cell tumors of the testes in pediatrics. Curr Opin Pediatr 2012;24(4):518–522.
89. Young RH. Sex cord-stromal tumors of the ovary and testis: their similarities and differences with consideration of selected problems. Modern Pathol 2005;18(suppl 2):S81–S98.
90. Liu P, Thorner P. Sonographic appearance of Sertoli cell tumour: with pathologic correlation. Pediatr Radiol 1993;23(2):127–128.
91. Hanson JA, Ambaye AB. Adult testicular granulosa cell tumor: a review of the literature for clinicopathologic predictors of malignancy. Arch Pathol Lab Med 2011;135(1):143–146.
92. Tsitouridis I, Maskalidis C, Sdrolia A, Pervana S, Pazarli E, Kariki EP. Adult type granulosa cell tumor of the testis: radiological evaluation and review of the literature. Turk J Urol 2014;40(2):115–119.
93. Zicherman JM, Weissman D, Gribbin C, Epstein R. Primary diffuse large B-cell lymphoma of the epididymis and testis. RadioGraphics 2005;25(1):243–248.
94. Shahab N, Doll DC. Testicular lymphoma. Semin Oncol 1999;26(3):259–269.
95. Liu KL, Chang CC, Huang KH, Tsang YM, Chen SJ. Imaging diagnosis of testicular lymphoma. Abdom Imaging 2006;31(5):610–612.